Modeling of Circadian Rhythms: Robust Temperature Compensation in *Drosophila melanogaster* and Testable Hypotheses in *Neurospora crassa*

Christian I. Hong

Dissertation submitted to the faculty of Virginia Polytechnic Institute and State University in partial fulfillment of the requirements for the degree of

Doctor of Philosophy
in
Biology

John J. Tyson, Chair
Robert Rogers
Jill C. Sible
Kimberly Forsten Williams
Edward J. Wojcik

December 3rd, 2003
Blacksburg, VA

Keywords: Circadian rhythms, modeling, temperature compensation

Modeling of Circadian Rhythms: Robust Temperature Compensation in *Drosophila melanogaster* and Testable Hypotheses in *Neurospora crassa*

Christian I. Hong

(Abstract)

Circadian rhythms are periodic physiological events that recur about every 24 hours. The word circadian derives from the Latin words *circa* "about" and *dies* "day". The importance of circadian rhythms is well recognized in many different organisms' survival as well as in human physiology. It was in the 1950's that scientists demonstrated the existence of an endogenous biological clock, and that the clock is temperature compensated. However, the molecular mechanism of circadian rhythms began to come clear only after the discovery of the *period* (*per*) gene in *Drosophila melanogaster* in 1971, and the *frequency* (*frq*) gene in *Neurospora crassa* in 1973. Since the breakthrough discoveries of the *per* and *frq* genes and their mutants (short period mutants, per^S or frq^1, frq^2; and long period mutants per^L or frq^3, frq^7), molecular biologists have discovered other crucial components of the mechanism of circadian rhythms. Currently, there are about a dozen identified circadian genes in *Drosophila melanogaster*. The consensus idea of the mechanism is that it involves two-interlocked feedback loops largely based on transcription-translation controls. However, based on our mathematical models and analysis, we propose that there is also an autocatalytic effect based on proteolysis and stabilization of PER proteins. Based on the dynamics of multiple steady states and limit cycle oscillation, we propose an alternative mechanism for robust temperature compensation. We start with a simple model in order to understand the core dynamics of the clock mechanism, and move to a more comprehensive model. In both cases, we use bifurcation analysis as a tool to understand the dynamics of the system. With our model, we propose hypotheses to be tested in *Neurospora crassa*.

Acknowledgements

First of all, I would like to thank God for His grace and mercy. I cannot imagine a life without God and the love of Christ. I am deeply indebted to my advisor Dr. John Tyson. His excellence in teaching and research has guided me throughout all of my graduate years. Moreover, I learned patience and integrity from Dr. Tyson. I am also grateful to all of my committee members: Dr. Robert Rogers, Dr. Jill Sible, Dr. Kimberly Forsten Williams, and Dr. Edward Wojcik. Their interest in the project and encouragements were invaluable.

I am thankful for the great lab members (Dr. Kathy Chen, Dr. Andrea Ciliberto, Dr. Laurence Calzone, Emery Conrad, and Jason Zwolak), and friends in Budapest (Professor Bela Novak, Dr. Attila Csikasz-Nagy, and Dr. Bela Gyorffy). They are my wonderful colleagues and friends. God has also granted me with such great people through Korea Campus Crusade for Christ at Virginia Tech. Lastly, I would like to add a special thanks to Yong Song and Y.H.K. for keeping me to strive throughout this last semester at Virginia Tech.

I dedicate this dissertation to my parents: Mr. and Mrs. Yun Cho Hong and Jung Sook Hong. They traveled far from their home country for their children. They have sacrificed so much for us. I love you mom and dad.

Table of Contents

List of Figures

List of Tables

List of Equations

Chapter 1 Background of Circadian Rhythms

1.1 General Properties of Circadian Rhythms

The term circadian rhythm refers to a cycle of approximately one day because organisms have quite accurate periodic cycles, but not exactly 24 hours. Circadian rhythms can be observed in many different organisms ranging from blue green algae to mammals. Organisms have a remarkable ability to maintain endogenous rhythms close to 24 h in period at various temperatures, pH, salinity, etc. The characteristic properties of circadian rhythms are: endogenous periodic oscillations, phase shift by light, entrainment to external cues such as light, and temperature compensation. Each property plays an important role in the organism's response to the ubiquitous 24 h rhythm of the surrounding environment. In case of disruption (by mutation) of any one of these properties, an organism is compromised in its ability to survive.

From the 18th century, people have been aware of the endogenous nature of circadian rhythms [1]. Endogenous means that organisms maintain their rhythms close to 24 hours even in the absence of external cues such as light or temperature. Endogenous rhythms can be demonstrated by observing organisms' locomotor activities in constant conditions (i.e. in constant darkness or in dim light). Figure 1.1.1 indicates that humans have an endogenous rhythm of about 26 h. This person spent about six months in a cave, measuring his sleep and wake cycles. For better representation of the rhythms longer than 24 h, the figure is double plotted with horizontal bars indicating the subject's sleep activities.

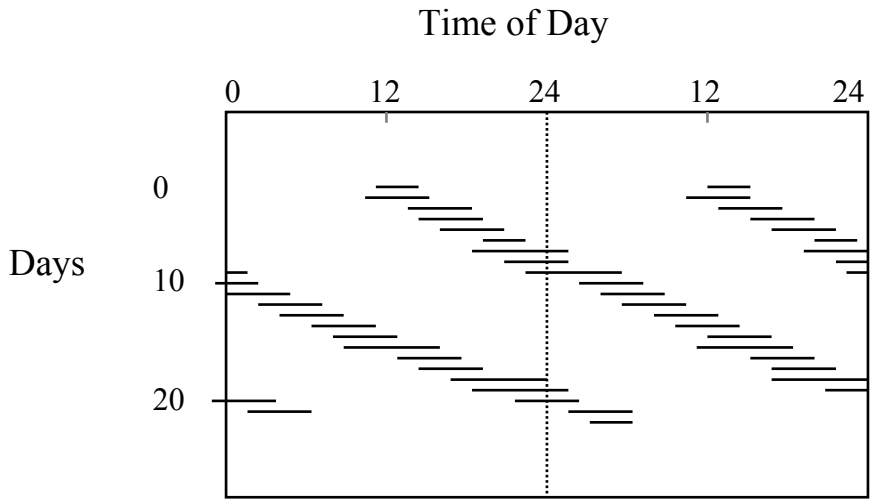

Figure 1.1.1 Siffre's sleep-wake cycles in a cave

Michael Siffre spent six months alone in a cave, measuring his sleep-wake cycles [2]. The graph is double-plotted, and horizontal bars indicate his sleep activities.

Endogenous rhythms are phase shifted upon a pulse of light in constant darkness. Organisms are put into constant darkness, and then exposed to a pulse of light. Afterwards, the new phase created by the light pulse is measured in comparison with the old phase. The new phase may show a delay or advance relative to the old phase, or no phase difference, depending on the timing of the light pulse. If the light pulse is given during the subjective day, when the organism is used to seeing the light, the pulse of light during those hours does not cause a change of phase (defined as dead zone). However, a light pulse given during the late subjective night causes a phase advance, because the organism responds to the light pulse by starting its activity early. Conversely, if the light pulse is given during the early subjective night, the organism's phase is delayed. Phase shifts are conveniently measured by phase response curves (Fig. 1.1.2).

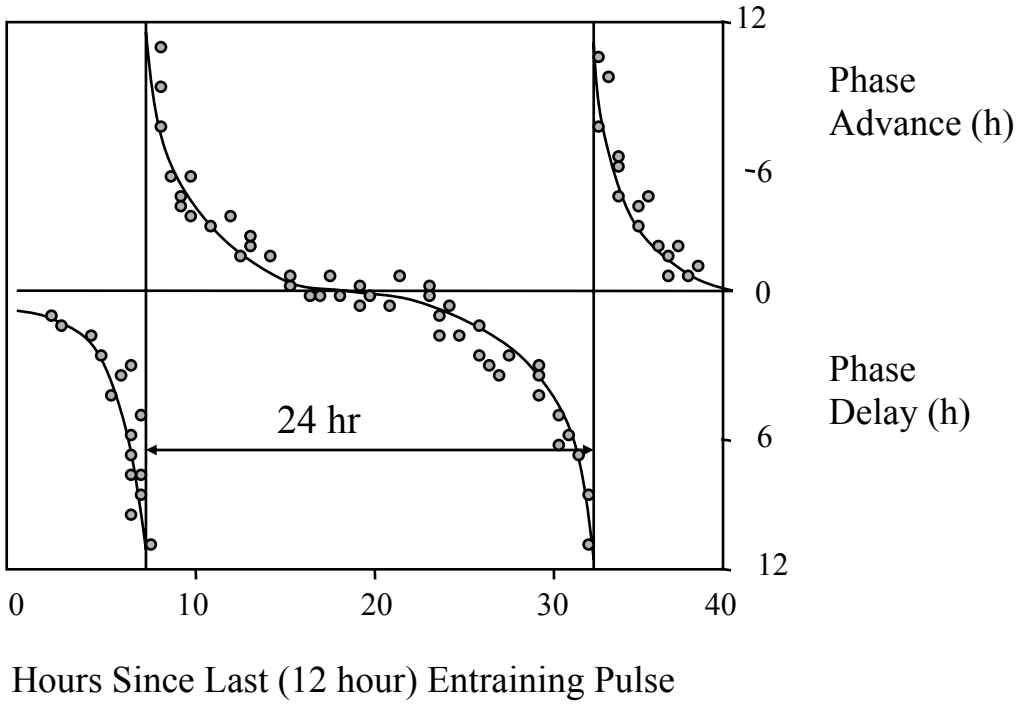

Figure 1.1.2 Phase response curve in *Drosophila pseudoosbscura* [3]
Fruit flies were entrained to 12 h light and 12 h dark cycles, and then put into constant darkness. In constant darkness, a 15 min light pulse (500 lux) was applied resulting in a phase-shift, as plotted in the graph, depending the timing of the pulse.

Circadian rhythms are entrained to external light cues such as light or temperature. Humans have an endogenous rhythm of 25-26 hours, *Neurospora crassa* has a rhythm of about 22 hours, and *Drosophila melanogaster* has a rhythm of about 24 hours. Endogenous rhythms with periods close to 24 hours can be entrained to the light and dark cycles that are imposed by the rotation of the earth. An organism's biological clock is synchronized to local time. Synchronization is possible only in a limited range of external Zeitgeber period (external time giver different from endogenous rhythms); the range of synchronization generally inreases with the magnitude of illumination.

The last and possibly most intriguing property of circadian rhythms is temperature compensation. The period of oscillation is quite stable over a wide range of temperatures [4]. Figure 1.1.3 denotes temperature compensated mobility rhythms of *Euglena gracilis* [5]. There is only a minor change in the period of oscillation over a large (15°C) temperature range. This is a remarkable property of circadian rhythms,

because chemical kinetics tells us that in general, if there is a 10°C increase in temperature, there is an increase of rate of kinetic reactions by a factor of two. In an attempt to explain temperature compensation of circadian rhythms, it is possible that reactions that decrease circadian period are exactly balanced by reactions that increase circadian period over a broad temperature range [6]. However, it is also quite difficult to imagine how this balance could be stable in the presence of mutation.

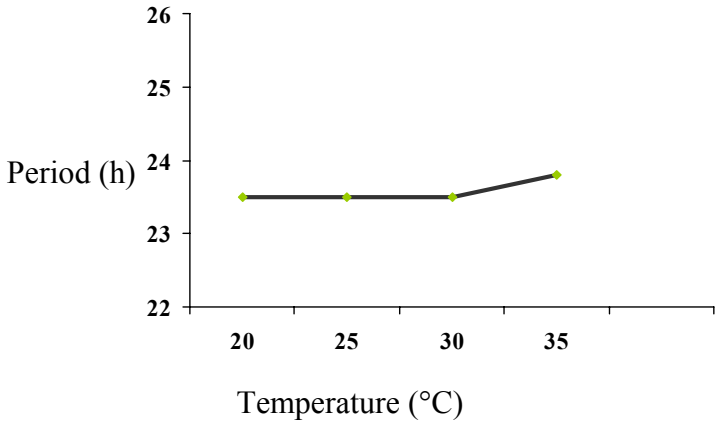

Figure 1.1.3 Temperature compensation of *Euglena gracilis*
The circadian rhythm of mobility of *Euglena gracilis* is measured in different temperature ranges. As the graph indicates, there is only a slight increase of the period over 15°C of temperature change.

Previously, the mechanism of circadian rhythms has been modeled mostly by stable limit cycle oscillators driven by a time-delayed negative feedback loop [7-14]. Models solely based on stable limit cycle oscillator naturally account for three of the above properties by the oscillator's generic nature (endogenous rhythms, entrainment, and phase-shift). However, these models suffer from sensitive period changes upon parameter variations. Therefore, time-delayed negative feedback oscillators wouldn't be suitable for accounting for the property of temperature compensation, because temperature induced increase of kinetic parameters in the system are expected to alter the period of the oscillation. Intrigued by these facts, we propose a model in which a

temperature compensation mechanism is embedded in the control system, and specifically generates robust circadian rhythms.

1.2 Molecular Biology of Circadian Rhythms in *Drosophila melanogaster*

A breakthrough of molecular biology of circadian rhythms occurred in 1971 when Konopka and Benzer isolated a novel circadian gene, *period* (*per*), in *Drosophila melanogaster* [15]. They identified a short period mutant, per^S, a long period mutant per^L, and an arrhythmic mutant, per^0. The wild-type flies have both eclosion and locomotor activities of about 24 hours, whereas mutant flies may have a shorter or longer period (e.g., 19 h in per^S and 28 h in per^L). Molecular cloning and sequencing in later years indicated that both per^S and per^L mutants had single missense mutations in *per* gene [16]. However, there is a critical difference between per^S and per^L in the location of mutations. The per^L mutation is located within the PAS (DNA binding domain: PER, ARNT, SIM) domain, which mediates dimerization of PERIOD (PER) protein as well as the interactions with its transcription factors, dCLOCK (dCLK) and CYCLE (CYC) [16-21]. Hence, per^L mutation affects PAS-mediated interactions, but per^S mutation does not interrupt the dimerization. The per^0 mutation codes for a nonfunctional PER proteins, and it abolishes the rhythm. The levels of *per* mRNA and PER protein oscillate with approximately 24 hour period, which directly reflects the physiological rhythms of fruit flies [22, 23]. The peak level of PER protein follows *per* mRNA with a time lag of about 4-6 h [24, 25]. This unusually long delay between the transcription and translation of PER indicates that there are post-transcriptional and/or post-translational processes involved in this dynamical system. Indeed, there is evidence where TIMELESS (TIM) protein stabilizes *per* mRNA by an unknown mechanism [26], and PER gets progressively phosphorylated by DOUBLETIME (DBT) protein [27-29], which we will discuss in detail. PER is a nuclear protein and inhibits its own synthesis by interacting with its transcription factors, dCLK and CYC via PAS domain.

Another novel component that was identified after PER, in 1994, is TIM protein [30, 31]. The levels of *tim* mRNA and TIM protein oscillate parallel to *per* mRNA and PER protein, and TIM exists in 1:1 ratio with PER [22, 32]. However, they seem to have different kinetics on the decreasing slope of their oscillations [23]. There are several *tim* mutants. The tim^{01} mutant encodes a truncated protein, and is considered as a non-functional, null mutant. The fruit flies' behavioral and eclosion rhythms are lost

in tim^{01} mutant [30]. In addition, PER is blocked from entering the nucleus [33], which results in an arrhythmic, low level of *per* mRNA. Therefore, TIM is necessary for nuclear translocation of PER. TIM physically binds with PER and they enter into the nucleus during early evening [32, 34, 35]. PER contains a cytoplasmic localization domain (CLD), which blocks its own nuclear entry, and TIM seems to hide PER CLD in such a way that PER gets transported into the nucleus [36, 37]. In *per* CLD deletion mutant (PERΔCLD), PER enters into the nucleus in the absence of TIM, and is functional in inhibiting its own synthesis. Similar to *per* mutants, there are long-period and short period mutants (tim^{UL}, tim^{SL} respectively) [38].

TIM is progressively phosphorylated by a kinase, SHAGGY (SGG) [39]. SGG encodes the *Drosophila* orthologs of glycogen synthase kinase-3 (GSK-3), and is essential for development of the fruit fly. Overexpression of *sgg* (sgg^{ov}) results in hyperphosphorylation of TIM, and is linked to premature nuclear localization of TIM [39]. Earlier entry of TIM results in short period phenotypes. By contrast, a reduction of *sgg* (sgg^{10}) activity results in a hypophosphorylated form of TIM, and lengthens the period to 26 h due to delayed nuclear entry of TIM [39].

TIM is also involved with another protein called CRYPTOCHROME (CRY) in a crucial part of the circadian rhythm: entrainment and phase shift by light. CRY is a clock specific photoreceptor, which belongs to a family of blue light receptor flavoproteins [40]. Upon exposure to light, CRY is thought to physically associate with TIM, and to target TIM to a proteosome dependent degradation pathway [41-44]. Because TIM directly affects the nuclear transport of PER, its degradation would have an acute effect on PER oscillations. In turn, this dynamical perturbation appears as phase advances and phase delays, depending on the amount and the location of TIM (cytoplasmic or nuclear) during the light pulse. In cry^{b} mutation (a missense mutation at a flavin-binding residue), TIM seems to be stable even in the light, and results in arrhythmic photoreceptor cells but unaffected lateral neurons in the brain [44]. Detailed interactions of TIM and CRY, and the proteolysis pathway need further investigation.

PER and TIM are known to negatively regulate transcription factors, CYC and dCLK. CYC and dCLK physically bind together and interact with *per* E-box sites [45, 46]. These, in turn, activate the transcription of *per* and *tim* [20]. Therefore, PER and TIM inhibit their own synthesis by down-regulating CYC and dCLK. The level of CYC

is constant throughout the cycle, while the level of dCLK oscillates in anti-phase to PER and TIM oscillations [47]. dCLK is phosphorylated in the process, but the role of phosphorylation on dCLK is still unknown [19, 48]. Both *cyc* and *dClk* mutants, cyc^0/cyc^0 and *Jrk* respectively, are arrhythmic resulting in low levels of *per* and *tim* mRNAs as well as PER and TIM proteins [18, 21]. Moreover, these mutants result in peak levels of *dClk* mRNA, which suggests that dCLK negatively inhibits its own synthesis [49].

PER is progressively phosphorylated by casein kinase I ε, DBT [27, 28]. Upon phosphorylation, PER is targeted to a protein degradation machinery. The activity of DBT determines the turnover of PER, which is reflected in the period of the rhythm. Increased activity of DBT in dbt^S mutant, hyperphosphorylates PER and shortens the period to 18 h, while its decreased activity in dbt^L mutant hypophosphorylates PER and lengthens the period to 28 h. Although the level of DBT does not oscillate, its activity may be regulated in circadian manner by binding to PER and TIM complex and translocating with them into the nucleus [29]. DBT is unable to down-regulate PER, because PER is in its stable form with TIM. Once DBT is in the nucleus, it would phosphorylate and trigger degradation of monomeric PER.

There are two additional components to this already complicated machinery: VRILLE (VRI) and Par Domain Protein 1 (PDP1) [50, 51]. Both of these proteins contain a highly conserved DNA binding domain, bZIP, and they compete with each other to bind the same promoter in *dClk* [51]. VRI oscillates in phase with PER and TIM, and is activated by transcription factors, dCLK and CYC [50]. *vri* mRNA level is high in tim^{01} mutant, which suggests that PER and TIM down-regulate VRI, even though it is still not known whether this is a direct or indirect inhibition via dCLK and CYC.

PDP1 also oscillates but with a slightly different phase than PER and TIM. PDP1 follows PER, TIM, and VRI delayed by about 4 h. It is also an essential component in the clock mechanism, in the sense that oscillation is blocked in $Pdp1^{P205}$ mutant [51]. PDP1 is activated by dCLK and CYC, and inhibited by PER and TIM as well. However, PDP1 seems to positively regulate the level of dCLK, because it shows a low level of *dClk* in $Pdp1^{P205}$ mutant. The antagonistic effects of VRI and PDP1 bring another level of complexity into the system.

1.3 Big Picture Put Together

In this section, I will summarize what I put together in the molecular biology section (1.2), and talk about what is the current idea of circadian rhythms. The consensus regarding circadian rhythms in *Drosophila melanogaster* is that it involves two interlocked feedback loops, which makes a robust oscillator.

The first feedback loop involves a negative feedback mechanism of PER and TIM proteins, where PER proteins bind to transcription factors, dCLK and CYC, and inhibit the transcription of both PER and TIM. PER and TIM proteins are progressively phosphorylated by DBT and SGG proteins, respectively. DBT binds to PER and progressively phosphorylates PER, and triggers fast degradation of monomeric PER proteins. The dimeric form of PER (present in low concentration), and its complex with TIM seem to be less susceptible for phosphorylation by DBT and therefore are stable. DBT bound to PER enters into the nucleus, and seems to function in PER turnover after its dissociation from the complex. SGG phosphorylates TIM and facilitates nuclear transport of TIM, although the mechanism is still not clear. Once PER is in the nucleus, it binds to the transcription factors, dCLK and CYC, via PAS domain and inhibits its own transcription. Light plays a role through a photoreceptor protein CRY. CRY is down-regulated by light, and the dissociation of TIM from CRY in the presence of light seems to put TIM through a ubiquitin-mediated degradation pathway. In this context, degradation of TIM upon the light pulse would create either phase delay or an advance depending on the time of the pulse.

The second feedback loop involves transcription factors, dCLK and CYC, PDP1 and VRI. dCLK and CYC activate transcription of both PDP1 and VRI, along with PER and TIM. PDP1 positively regulates dCLK and CYC while VRI negatively regulates them. A simple schematic diagram of interlocked feedback is illustrated in figure 1.3.1. These interlocked feedback loops introduce complicated dynamical behaviors in the system of biochemical oscillator.

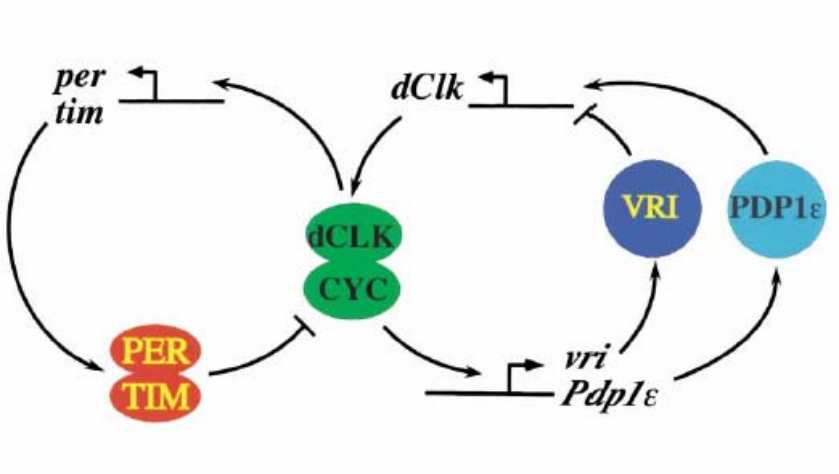

Figure 1.3.1 Interlocked feedback mechanism [51]

1.4 Mathematical Models

Intuition is insufficient to understand fully a complex control system such as circadian rhythms. A mathematical representation (i.e. differential equations) of such mechanism is needed to understand the dynamical properties of the control system. From early 1970s to 1980s, there were efforts to model circadian rhythms [52-54]. These early models were phenomenological models, where they used mathematics without any basis of molecular biology, in order to explain observed physiological behaviors of circadian rhythms (i.e. sleep and wake cycles, phase shift, etc.). In the 1990s there has been a great acceleration in discoveries of the genetic components of circadian rhythms. However, a group in Harvard continues to use the Van der Pol oscillator to explain observed behaviors of human sleep wake cycles [7,9].

In 1995, Albert Goldbeter presented the first mathematical model of circadian rhythms based on molecular findings in *Drosophila melanogaster* [8]. At the time, the only known component of clock mechanism was PER protein, and its known function of self inhibition. Goldbeter used time-delayed negative feedback loop represented by multiple phosphorylation of PER proteins before entering into the nucleus, and inhibition on *per* transcriptions exerted by nuclear PER proteins. Goldbeter and his group used this model as a foundation to develop more comprehensive models [10] in fruit flies as well as in mammals [11].

In the late 1990s, many groups around the world began to publish models of circadian rhythms. A group in Japan reported a model of the interlocked feedback loop as described in figure 1.3.1 [14]. Another lab in Texas, presented models for both fruit flies' and bread molds' circadian rhythms with explicit time-delays in the system [12]. Peter Ruoff in Norway was particularly interested in the property of temperature compensation in biological clock of *Neurospora crassa* [6]. Ruoff used Goodwin's model to generate a biochemical oscillator, and indicated that the period of the system is largely effected by the changes of degradation rate of proteins. All of these models based on molecular mechanisms employ a stable limit cycle oscillator generated by time-delayed negative feedback loop as means of creating a period of about 24 h.

1.5 Goals, Tools, and Hypotheses

Our goal is to make a plausible model of the circadian rhythm mechanism based on current revelations of molecular biology. A model is built by converting a schematic diagram of the control system into a set of ordinary differential equations. Then, the model is simulated and analyzed by software XPPAUTO [55]. XPPAUTO is divided into two parts: XPP and AUTO. Nonlinear differential equations can be solved in XPP with different integrators (i.e. Stiff, Gear, Euler, etc.). Some of the functions of XPP are to compute solutions for differential equations and eigenvalues at steady states. A simple model of two equations can be even plotted in a phase plane portrait, where the user can observe changes of nullclines of two variables upon variations of parameter values in the system. Phase plane analysis is useful to understand dynamical properties of a model with two equations.

AUTO is a program for numerical bifurcation analysis. This tool allows XPP to grab a steady state of a system, and tracks the steady state as a function of a kinetic parameter. As AUTO follows the steady state of the system, it identifies bifurcation points (where the stability of the system changes) and labels them according to the type of bifurcation. For instance, AUTO recognizes Hopf bifurcation point (where a family of periodic orbits is born), and labels it as HB. Furthermore, Hopf bifurcation can be followed in two parameter space indicating a region of a oscillatory domain in two parameter space.

Using these tools, I have studied many alternative models of the mechanism of circadian rhythms in fruit flies, and identified two hypotheses: 1) the existence of autocatalysis in the system based on the mechanism of proteolysis of PER protein, and 2) a robust temperature compensation mechanism based on the periodic resetting hypothesis as an alternative to the limit cycle hypothesis. Both of hypotheses are discussed and analyzed for a simple model (Chapters 2.1 and 2.2), and then applied to a more comprehensive model (Chapter 3.1). Our mathematical models satisfy all four properties of circadian rhythms and generate experimentally testable hypotheses (Chapter 4.3).

Chapter 2 Simple Model of Circadian Rhythms in *Drosophila melanogaster*

2.1 Simple Model and Limit Cycle Oscillator

The consensus picture from section 1.3 can be described in a schematic diagram (Fig. 2.1.1), which includes all of the known components. If we convert this model into a set of differential equations, we would have a system of 16 variables. Although it is possible to put these equations into a computer and run simulations, we would be lost in the ample region of parameter space. In order to have a clear understanding and to grasp the core mechanism of the system, we need to reduce the model into a handful of components. In 1999, we proposed a simple model (Fig. 2.1.2) of circadian rhythms based on dimerization and proteolysis of PER and TIM [13]. First of all, in order to derive a simple model, we only concentrated on the first loop of interlocked feedback loops. Moreover, the story of interlocked feedback loops was not established at the time of our investigation of our simple model.

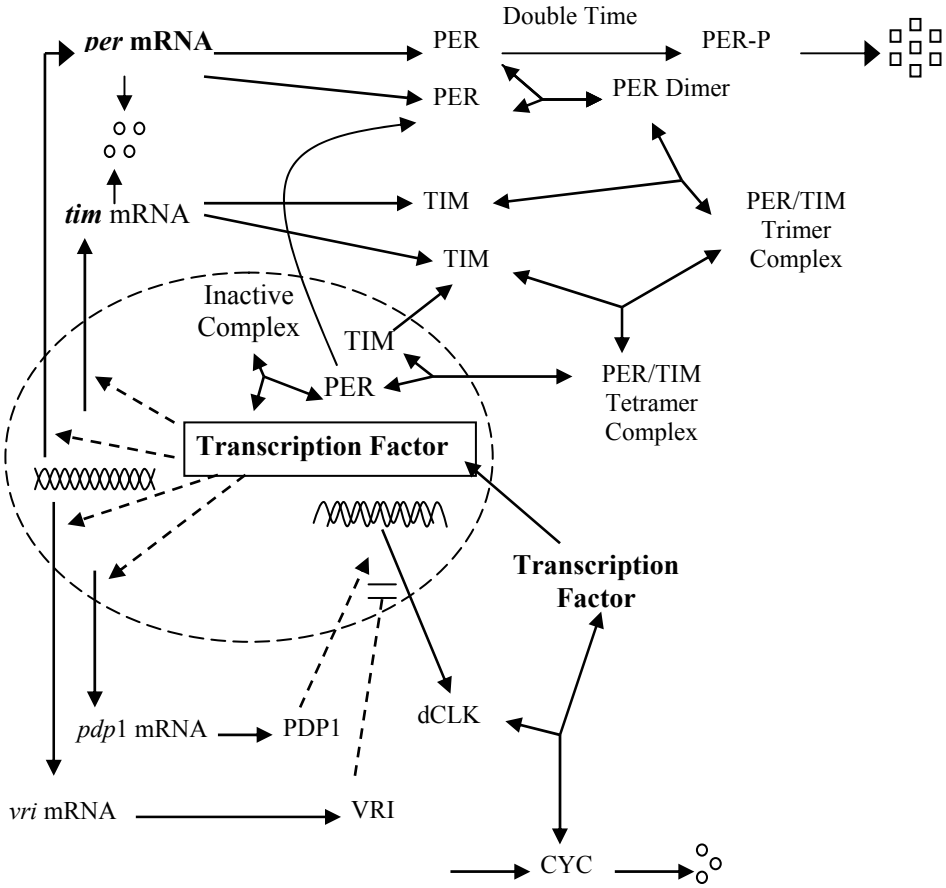

Figure 2.1.1 Comprehensive model of circadian rhythms in *Drosophila melanogaster*

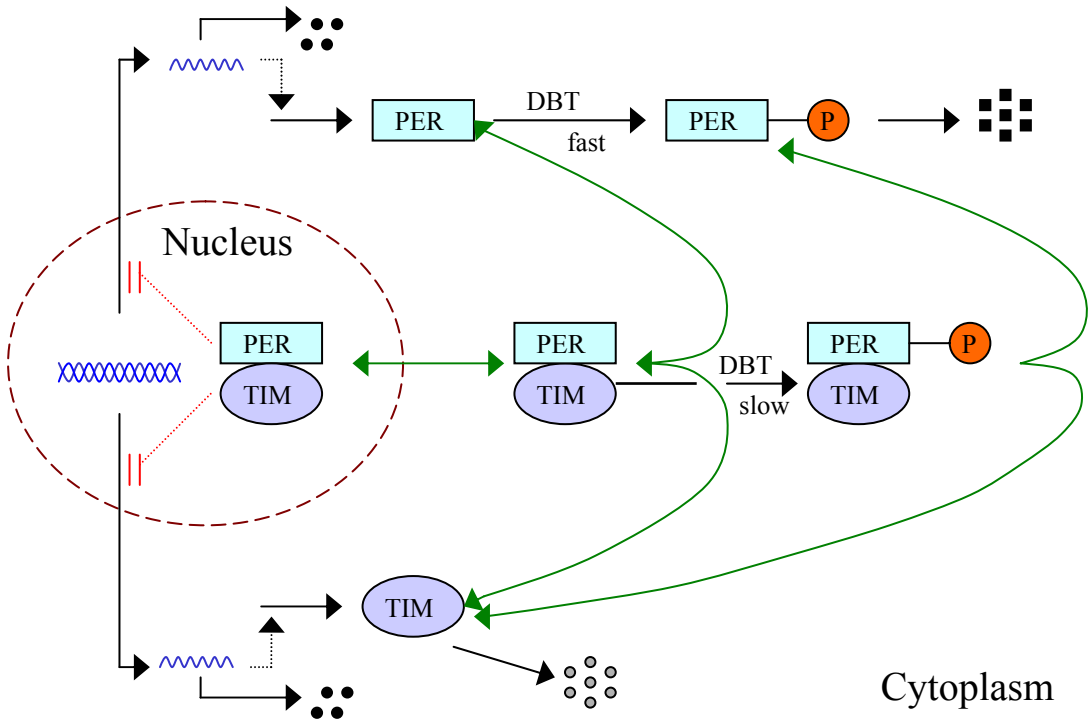

Figure 2.1.2 Reduced comprehensive model

The dynamical kinetics involved with DBT (phosphorylation and subsequent degradation of monomeric PER) gave us a clue that there could be an autocatalytic process of PER accumulation. At low concentrations of PER proteins, most of them would be degraded by DBT related kinetics. However, as the level of PER increases, there is a shift of monomeric PER to its dimeric form, which is more stable than the monomeric form. In other words, as the PER concentration rises, there is an even greater chance to form a complex either with itself (homodimerization) or with TIM (heterodimerization). This dimerization stabilizes PER so that PER can escape from DBT induced proteolysis. The rate of degradation of PER does not increase proportionally with the total concentration of PER. Hence, PER inhibits its own degradation, which introduces positive feedback (autocatalysis) into the nonlinear dynamical system.

The reduced mechanism in Fig. 2.1.2 summarizes the properties of PER, TIM, and DBT, and their negative and positive feedback loops. This mechanism can be converted into six differential equations following the rate of changes of *per* and *tim*

mRNA, PER and TIM monomeric proteins, PER-TIM heterodimer in the cytoplasm and in the nucleus. Even though this is already a reduced model from figure 2.1.1, it is still not trivial to understand the role of the positive feedback mechanism in this complicated system. Hence, we further reduced this model to a simpler picture by lumping together *per* and *tim* mRNA, and PER and TIM proteins, knowing that they follow similar time courses. We also assumed that dimer formation and nuclear entry are fast. The simplified model (Fig. 2.1.3) is converted into the following three differential equations:

[Equation 2.1.1] $$\frac{dM}{dt} = \frac{v_m}{1+\left(\frac{P_2}{P_{crit}}\right)^2} - k_m M$$

[Equation 2.1.2] $$\frac{dP_1}{dt} = v_p M - \frac{k_{p1} P_1}{J_p + P_1 + 2P_2} - k_{p3} P_1 - 2k_a P_1^2 + 2k_d P_2$$

[Equation 2.1.3] $$\frac{dP_2}{dt} = k_a P_1^2 - k_d P_2 - \frac{k_{p2} P_2}{J_p + P_1 + 2P_2} - k_{p3} P_2$$

The rate of change of [mRNA], [protein], and [dimerized protein] are denoted as dM/dt, dP_1/dt, and dP_2/dt, respectively. The message is transcribed with a maximal rate of v_m and inhibited by PER/TIM heterodimers, and proportionally degraded (k_m) depending on its own concentration. We assume a Hill exponent of two, which represents some cooperativity for the inhibition of the negative feedback loop. This cooperativity is not essential for the limit cycle oscillations, but the system is more robust when the exponent is two. Monomeric proteins are synthesized proportionally with the concentration of mRNA, and degraded or associated with other monomeric proteins to form dimers. Dimers are formed from the association of monomers, and can also be degraded or lost by dissociation. Both monomers and dimers are subject to phosphorylation by DBT, and degrade upon phosphorylation. However, based on experimental evidence [27, 28], we assume that P_1 is more susceptible to phosphorylation and degrades rapidly, and P_2 is less susceptible to phosphorylation ($k_{p1} >> k_{p2}$). The DBT-catalyzed reaction is described by saturable kinetics, which is

essential for our positive feedback to work properly. Also note that P_2 is a competitive inhibitor of P_1 phosphorylation.

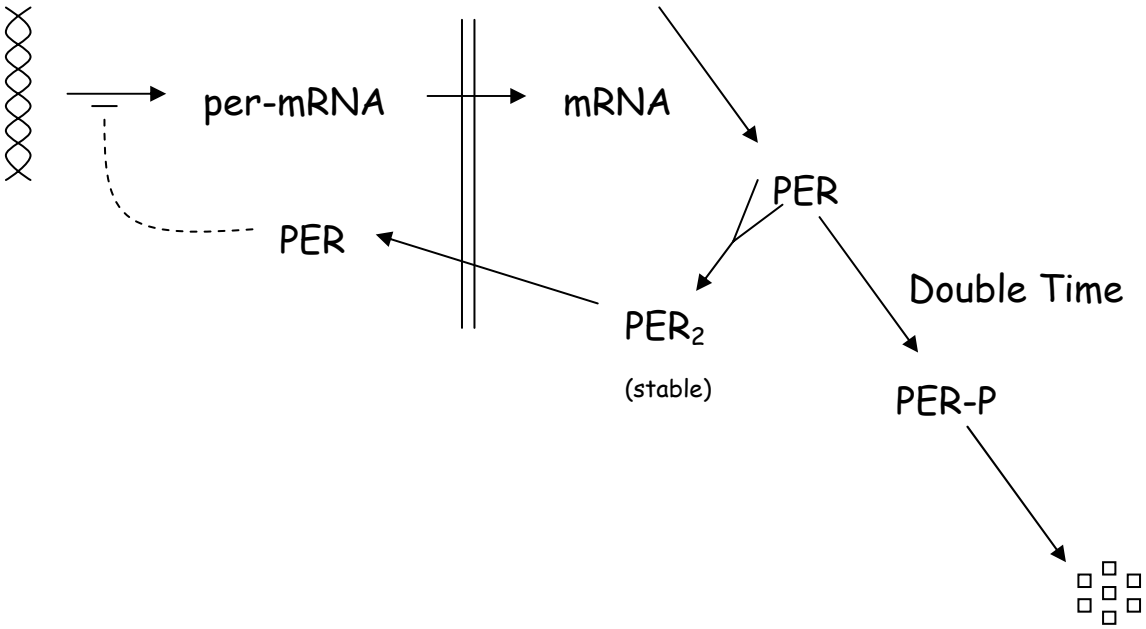

Figure 2.1.3 Simplified model of circadian rhythms in *Drosophila melanogaster*

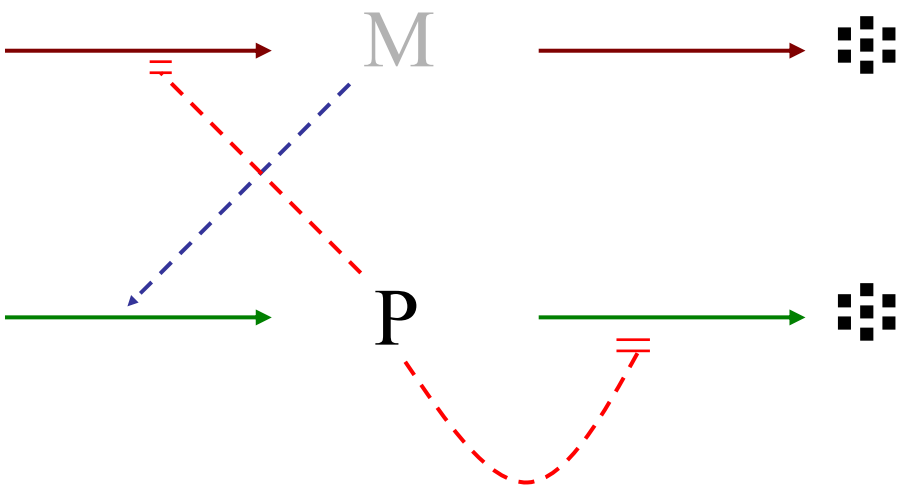

Figure 2.1.4 Simple schematic diagram of positive and negative feedback loops

This set of three differential equations is further reduced to two differential equations by expressing P_1 and P_2 as functions of total protein ($P_t = P_1 + 2P_2$). If dimerization reactions are fast enough, P_1 and P_2 will always be in equilibrium with each other. If we let $K_{eq} = \frac{P_2}{P_1^2}$ and $q = \frac{P_1}{P_t}$, we can get $P_2 = \frac{1}{2}(1-q)P_t$, where $q = \frac{2}{1+\sqrt{1+8K_{eq}P_t}}$. Based on these facts, we can reduce the original set of three differential equations into a pair of nonlinear ordinary differential equations:

[Equation 2.1.4] $$\frac{dM}{dt} = \frac{v_m}{1+\left(\frac{P_t(1-q)}{2P_{crit}}\right)^2} - k_m M$$

[Equation 2.1.5] $$\frac{dP_t}{dt} = v_p M - \frac{k_{p1}' P_t q + k_{p2} P_t}{J_p + P_t} - k_{p3} P_t$$

where $k_{p1}' = k_{p1} - k_{p2}$, and k_{p2} is significantly smaller than k_{p1}. This system of two ordinary differential equations is diagrammed schematically in figure 2.1.4.

If we choose the right parameter values (Table 2.1.1), it is possible to generate a 24 h free-running cycle of mRNA and protein (Fig 2.1.5). The protein peak is delayed about 6-7 h after peak mRNA level. This result is somewhat different from the experimental observation that PER protein is delayed about 4-6 h after mRNA.

Table 2.1.1 Parameter values for circadian rhythm of wild-type fruit flies

Name	Value	Units *	E_a/RT #	Description
v_m	1	$C_m\ h^{-1}$	6	Maximum rate of synthesis of mRNA
k_m	0.1	h^{-1}	4	First-order rate const for mRNA degrad'n
v_p	0.5	$C_p\ C_m^{-1}\ h^{-1}$	6	Rate constant for translation of mRNA
$k_{p1'}$	10	$C_p\ h^{-1}$	6	V_{max} for monomer phosphorylation
k_{p2}	0.03	$C_p\ h^{-1}$	6	V_{max} for dimer phosphorylation
k_{p3}	0.1	h^{-1}	6	First-order rate const for proteolysis
K_{eq}	200	C_p^{-1}	-12	Equilibrium constant for dimerization
P_{crit}	0.1	C_p	6	Dimer concen at half-maximal transcr'n rate
J_p	0.05	C_p	-16	Michaelis constant for protein kinase (DBT)

* C_m and C_p represent characteristic concentrations for mRNA and protein, respectively.
# E_a is the activation energy of each rate constant or the standard enthalpy change for each equilibrium binding constant.

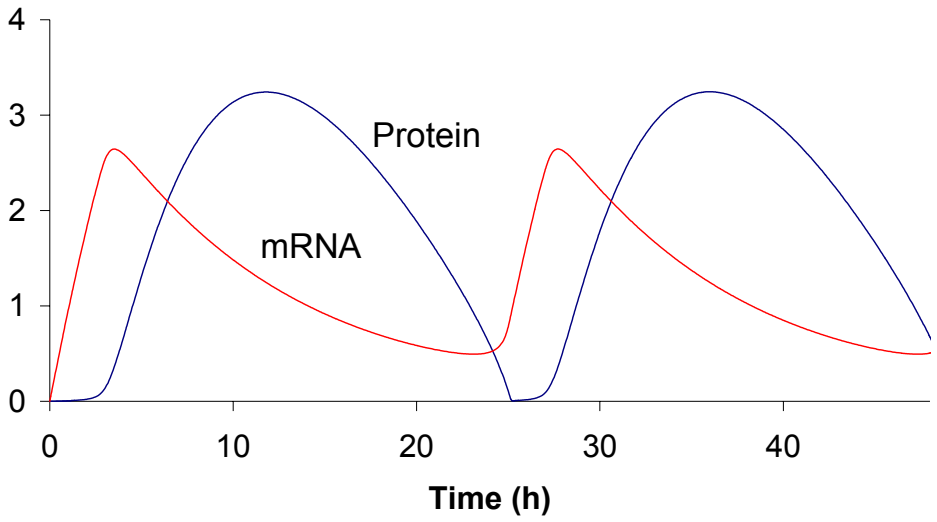

Figure 2.1.5 Oscillations of mRNA and protein

2.1.1 Phase Plane Analysis and Bifurcation Diagram

The importance of reducing the model to a pair of nonlinear ordinary differential equations is due to the fact that the simplicity of two-equation model provides a great advantage in phase plane analysis. The phase plane for equations 2.1.4 and 2.1.5, is the Cartesian coordinate system representing each of the variables, mRNA and total protein, respectively. The nullclines, or balance curves, are plotted in the phase plane. These are referred as balance curves, because M-nullcline represents where mRNA synthesis is balanced by its degradation, and likewise, P_t-nullcline represents balanced protein synthesis and degradation, and they are defined by the following equations:

$$\text{(M-nullcline)} \quad M = \frac{v_m}{k_m}\left[1+\left(\frac{P_t(1-q)}{2P_{crit}}\right)^2\right]^{-1}$$

$$\text{(P_t-nullcline)} \quad M = \frac{k_{p1}P_t q + k_{p2}P_t}{v_p(J_p+P_t)} + \frac{k_{p3}P_t}{v_p}$$

The phase plane portrait describes temporal behavior of the system based on the kinetic rate constants. Figure 2.1.6 depicts sigmoidal M-nullcline and N-shaped P_t-nullcline. Where these two nullclines intersect is denoted as a steady state of the system. This particular steady state is unstable, and the stable limit cycle oscillates around it (with the parameter set from Table 2.1.1). However, if we change parameter values (e.g., by mutation), the nullclines would move, thereby changing the portrait of the system. If we were to change the equilibrium-binding constant, K_{eq}, then we would see the change of P_t-nullcline according to the variations of K_{eq}. These changes in nullcline will trigger either a change in the period of oscillation, or the disappearance of the stable limit cycle (Fig. 2.1.7).

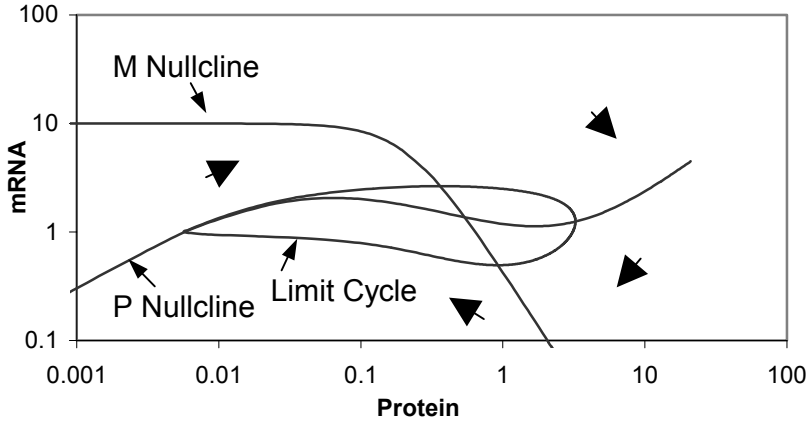

Figure 2.1.6 Phase plane portrait of mRNA and protein

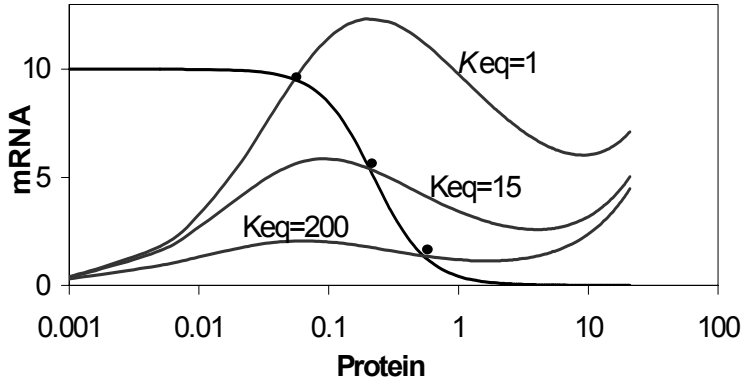

Figure 2.1.7 Steady state changes varying K_{eq}

A numerical bifurcation analysis of the model is used for further understanding of the system dynamics. Bifurcation analysis describes stability changes of the system upon variation of parameter values. For instance, in figure 2.1.8, we follow the steady-state level of total protein in a function of the phosphorylation-induced degradation rate constant of monomeric PER protein, k_{p1}. The solid lines represent stable steady states, and the dashed line represents an unstable steady state with stable limit cycle. Starting at low k_{p1}, the system is at a stable steady state with no oscillations, but as it crosses 6.16, it enters into a region of oscillatory domain with a stable limit cycle. As the steady state level crosses 46.48, it is drawn back to another stable steady state. The points where the stability of the steady state changes are called bifurcation points, which are labeled and categorized according to their unique characteristics. For example, we

see two Hopf bifurcation points in figure 2.1.8. As a bifurcation parameter changes through a Hopf bifurcation, a steady state changes stability and a family of small amplitude periodic solutions appear. The periodic solutions may be stable (supercritical Hopf bifurcation) or unstable (subcritical Hopf bifurcation). In figure 2.1.8, there is supercritical Hopf bifurcation at k_{p1}=6.16, and a subcritical Hopf bifurcation at k_{p1}=46.48, and the periodic solutions are part of a continuous one-parameter family of limit cycles.

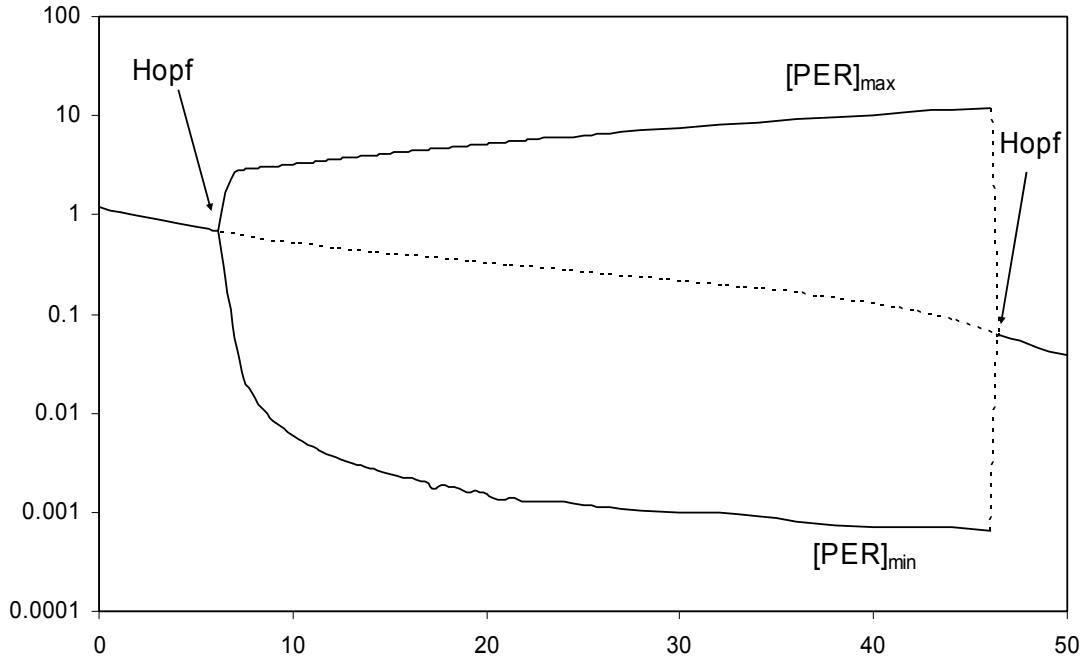

Figure 2.1.8 One parameter bifurcation diagram with parameter: k_{p1}

In figure 2.1.9, we follow the Hopf bifurcation in two parameter space: K_{eq} and k_{p1}. Within the U-shaped region, labeled as H for Hopf, the system is in the domain of stable limit cycle. As you can see in figure 2.1.9, for a robust oscillation, the model requires large values of K_{eq} and k_{p1}. We assume that the wild type resides in these large values of K_{eq} and k_{p1}, where the period of oscillation is close to 24 h and it is quite insensitive to temperature induced changes in parameters. However, at low values of K_{eq}, the period of oscillation is sensitive to both K_{eq} and k_{p1}. It is known that per^{L} mutant fails to interact with both PER and TIM proteins (decreasing K_{eq}), which leads to an increased period of oscillation with a disruption in temperature compensation.

2.1.2 Temperature Compensation, Phase Shift, and Entrainment

Our simple model employs a stable limit cycle oscillator, and due to the oscillator's generic nature, the period of the oscillation is sensitive to temperature induced parameter variations. In order to take this into account for temperature compensation in wild type and temperature dependence in *per*^{L} mutant, it was necessary to carefully balance each parameter in the model by assigning appropriate activation energies (Table 2.1.1 and Table 2.1.2).

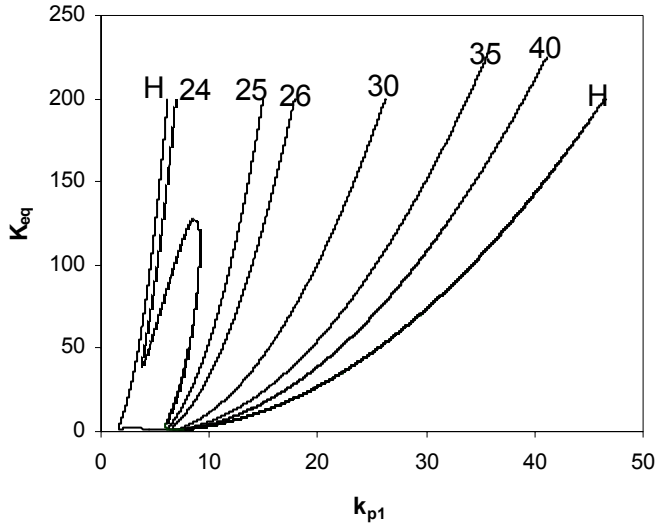

Figure 2.1.9 Two-parameter bifurcation: K_{eq} vs. k_{p1}

Table 2.1.2 Period of the endogenous rhythms of wild-type and mutant flies

Genotype	K_{eq}	Temp*	Period	Genotype#	k_{p1}	k_{p2}	Period
Wild type	245	20	24.2	dbt^{+} (1×)	10	0.03	24.2
	200	25	24.2	(2×)	15	0.06	24.4
	164	30	24.2	(3×)	20	0.09	25.7
per^{L}	18.4	20	26.5	dbt^{S}	10	0.3	17.6
	15.0	25	28.7	dbt^{+}	10	0.03	24.2
	12.3	30	30.5	dbt^{L}	10	0.003	25.2

*We assume that each parameter k varies with temperature according to $k(T) = k(298)\exp\left\{\varepsilon_a\left(1-\frac{298}{T}\right)\right\}$, with values for $k(298)$ and $\varepsilon_a = E_a/(0.592 \text{ kcal mol}^{-1})$ given in Table 2.1.1.

#$dbt^{+}(n\times)$ means n copies of the wild-type allele.

Other important properties of circadian rhythms are: phase shift by light pulses in constant darkness, and entrainment to external Zeigeber imposed by light and dark cycles. This model can account for phase shift properties of circadian rhythms in response to light pulses in constant darkness. Based on the evidence of TIM protein degradation upon light pulse, and thereby disrupted PER-TIM heterodimerization, we assume that light pulse reduces the equilibrium-binding rate constant, K_{eq}. With this assumption, we were able to generate typical phase response curves demonstrating phase delays and advances depending on the timing of light pulse (Fig. 2.1.10). The model was simulated with either 10 minutes or 30 minutes of reduced K_{eq} at different time intervals, which created perturbations in the system. After the timed pulse, the default value of K_{eq} was reapplied for the rest of the cycle, bringing the system back as before to constant darkness. The general shapes of phase response curves (PRCs) were qualitatively similar to PRCs obtained from experiments [3, 56]. In addition, figure

2.1.11 indicates that the model can be entrained to external Zeitgeber with a period different from 24 h within V-shaped entrainment band.

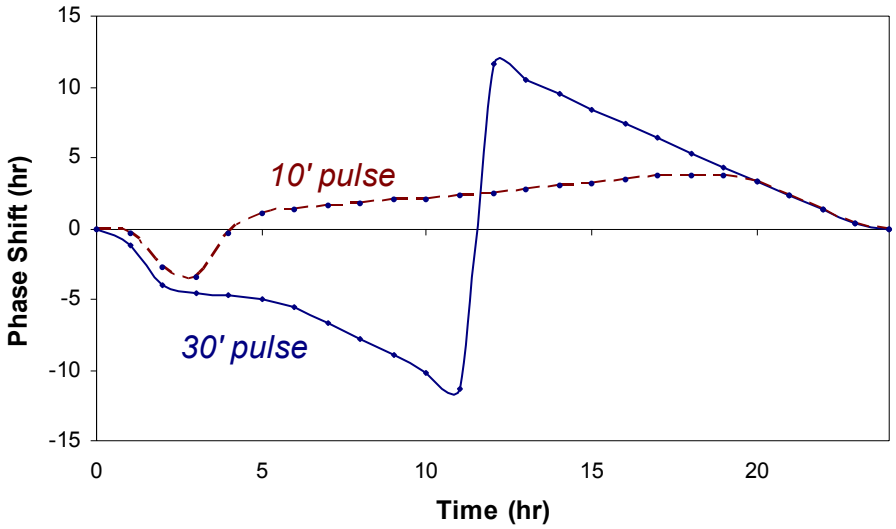

Figure 2.1.10 Phase response curves (PRC)

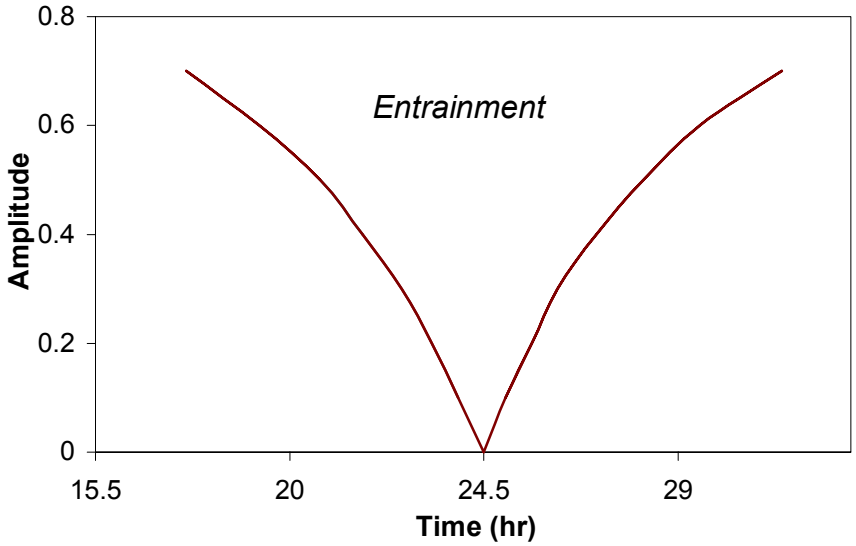

Figure 2.1.11 Entrainment band

2.1.3 Bifurcation Analysis

In order to explore the enriched dynamics generated by the positive feedback loop, we continued further bifurcation analysis in search of a new parameter set describing hysteresis with a region of multiple steady states. In figure 2.1.12, we follow the steady state of P_t as a function of the degradation rate of monomeric protein, k_{p1}. As k_{p1} decreases from its high value ($k_{p1}>11$), the system encounters three bifurcation points: two saddle node (SN) bifurcations and a Hopf bifurcation. The oscillations are born either at Hopf bifurcation or at SNIC (Saddle-Node on an Invariant Circle) bifurcation [57, 58]. Within the small window of k_{p1} ($8.05 < k_{p1} < 8.68$), there exists a region of multiple steady states where a stable and two unstable steady states coexist. We further followed these bifurcation points in two-parameter space as in figure 2.1.9 (Fig. 2.1.13). Figure 2.1.13 is significantly different from figure 2.1.9.

The SN bifurcation lie along two fold lines (black curves) that meet at a codimension two cusp bifurcation point, as expected [57]. The Hop bifurcation point in figure 2.1.12 lies on a locus of Hopf points (red curve) which ends tangentially on one of the fold lines, at a codimension two Takens-Bogdanow (TB) point [57]. Two parameter bifurcation diagram gives us a broader picture of the dynamical properties of the control system, but we will be using only one parameter bifurcation diagram in the remainder of the dissertation. In section 2.2, we will discuss how these bifurcation analyses are useful in proposing a new hypothesis of the mechanism of circadian rhythm.

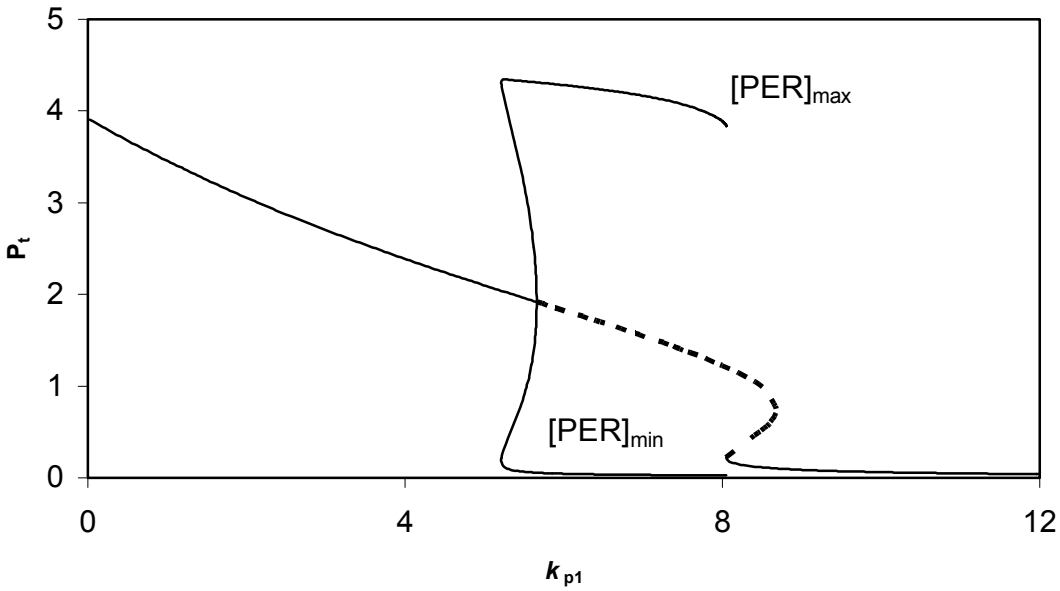

Figure 2.1.12 One parameter bifurcation with k_{p1}

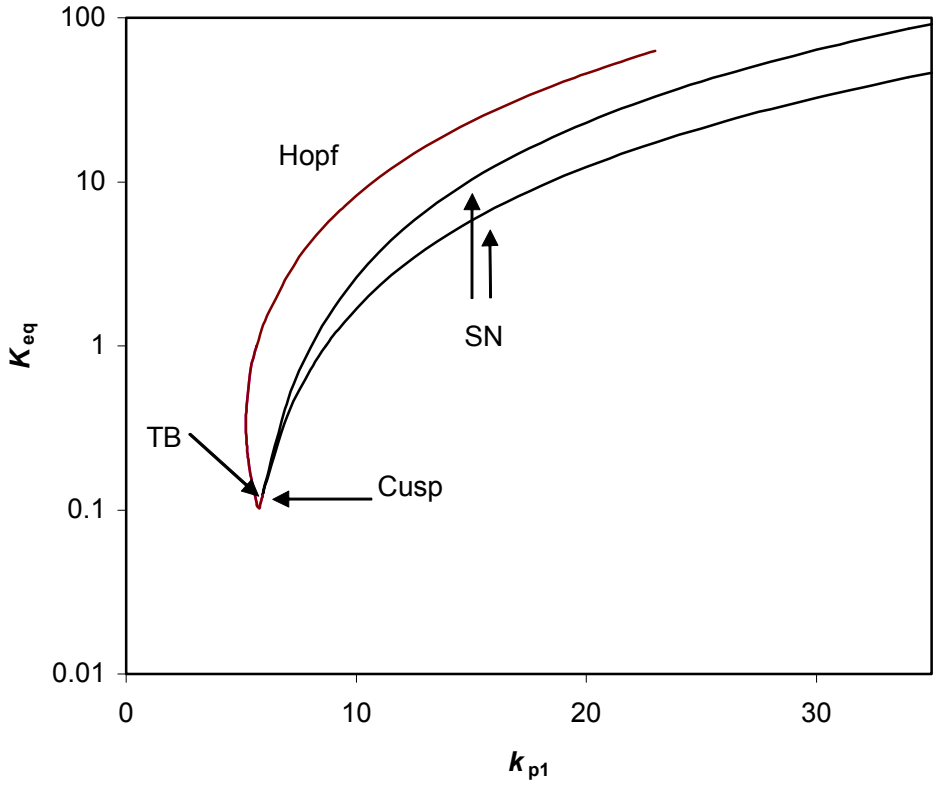

Figure 2.1.13 Two parameter bifurcation: K_{eq} vs. k_{p1}

2.2 Resetting hypothesis

Our simple model has shown that autocatalysis in the system in addition to the negative feedback loop may play a major role in generating a robust biological clock. Numerical bifurcation analysis of our simple model with a positive feedback loop revealed a region of multiple steady states with a different parameter set from Table 2.1.1 (Fig. 2.1.12). This is a generic picture that we would expect to see from the system containing an autocatalytic positive feedback signal. Based on our bifurcation analysis, we propose a resetting hypothesis: a biochemical oscillatory mechanism alternative to previous stable limit cycle oscillator hypotheses.

Our previous model with two equations is used to perform phase plane analysis. With a new parameter set (Fig. 2.2.1A), modified from our previous publication, we show phase plane portraits depend on the kinetic parameter of translational efficiency, v_p. At v_p=30, two nullclines (mRNA and protein) intersect, creating an unstable steady state with a stable limit cycle (Fig. 2.2.1A). As we decrease v_p by ten fold (v_p=3), we observe that these nullclines intersect at three different places with two unstable steady states and one stable steady state (Figure 2.2.1B). The latter case has a region of multiple steady states, and solutions are attracted to the stable steady state.

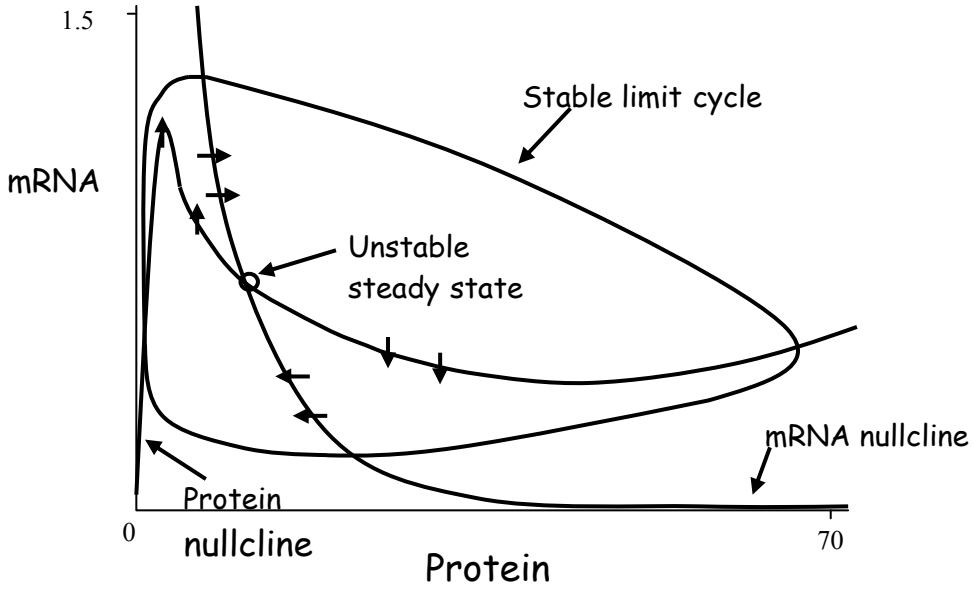

Figure 2.2.1A Schematic phase plane portrait at v_p = 30

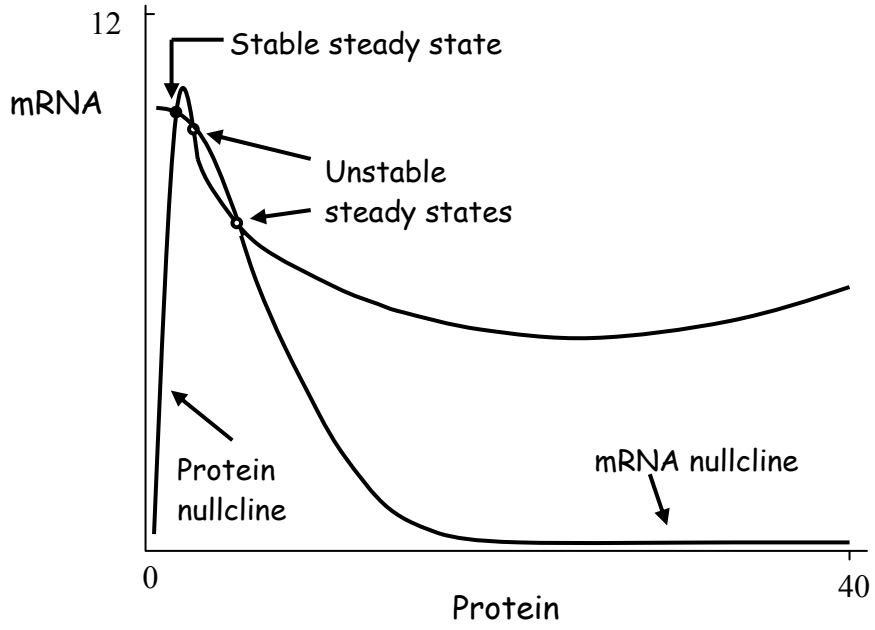

Figure 2.2.1B Schematic phase plane portrait at $v_p = 3$

A one-parameter bifurcation diagram (Fig. 2.2.2A) captures stability changes as a function of translational efficiency, v_p. This diagram shows an unstable steady state with a stable limit cycle at $v_p = 30$, and three steady states at $v_p = 3$ as indicated in the figure 2.2.1. In figure 2.2.2A, the solid lines represent stable steady states, and the dashed line represents unstable steady state. Oscillations are born either at a Hopf bifurcation ($v_p = 72$), with small amplitude, or at a SNIC bifurcation ($v_p = 3.28$) with large amplitude oscillations. The amplitude of the oscillation is denoted as $[PER]_{max}$ and $[PER]_{min}$ at a fixed value of v_p. The period of oscillation is quite insensitive to the changes of v_p ($7 < v_p < 72$), but increases to infinite period as v_p approaches the SNIC bifurcation (Fig. 2.2.2B). A region of multiple steady states ($2.98 < v_p < 3.28$) is denoted by hysteresis (the S-shaped curve), which creates a switch-like system.

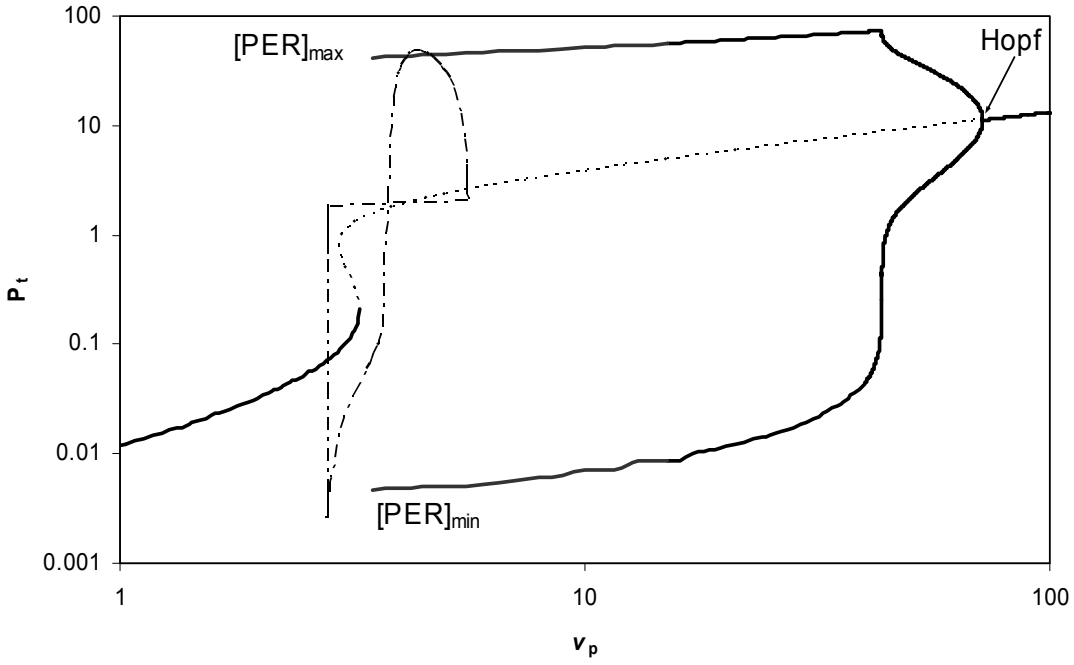

Figure 2.2.2A One parameter bifurcation diagram with v_p

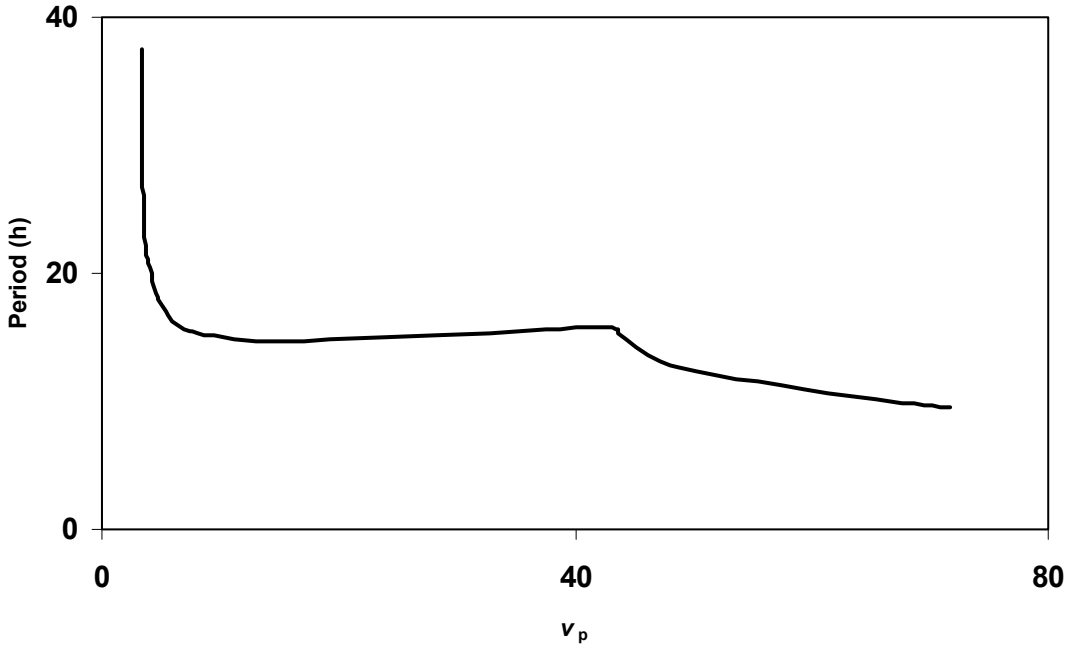

Figure 2.2.2B Period dependency in function of v_p

In order to explain the properties of circadian rhythms with such a model, it is natural to adopt the "limit cycle hypothesis," and choose a value of v_p in the region of oscillatory solutions, such as v_p =30. For the value of v_p, PER proteins execute periodic limit cycle oscillations between a maximal value ($[PER]_{max}$) and minimal value ($[PER]_{min}$), which denotes the amplitude of oscillation. This hypothesis, that the central control mechanism executes limit cycle oscillations, automatically accounts for the endogenous nature of the rhythms, for entrainment, and for phase response curves. But it is difficult to satisfy the property of temperature compensation with a limit cycle hypothesis. In general, the period of a limit cycle oscillator depends sensitively on all the kinetic parameters in the model, and the kinetic parameters are sensitive to temperature changes. If any one of these parameters is changed by a factor of two, the period of the oscillator will most likely shift far away from 24 hours.

Ruoff solved this problem by applying the Arrhenius equation, $k = A \cdot e^{-\frac{E_A}{RT}}$, for calculating different rate constants depending on different activation energies, and balancing the rate constants as shown in the equation below [6].

[Equation 2.2.1] $$\frac{\mathrm{d}Period}{\mathrm{d}Temp} = \sum_{params} \frac{\partial Period}{\partial param} \frac{\partial param}{\partial Temp} \cong 0$$

The period of the system is dependent on the parameters, and the parameters are dependent on temperature. Hence, by the chain rule, the derivative of Period with respect to Temperature is a sum of many terms. If the terms cancel out and the sum is close to zero, then the oscillator is temperature compensated. By appropriate choice of activation energies, it is always possible to satisfy this condition, but it is not a robust explanation of temperature compensation. It is not a robust in the sense that this sum is not likely to be zero in case of mutants, because mutations would likely disrupt the dependence of period on parameter values. When these coefficients change in arbitrary ways, the sum will no longer be zero, and the system will not be temperature compensated. On the contrary, there are temperature compensated mutants both in *Neurospora crassa* (frq^1) as well as in *Drosophila melanogaster* (tim^{S2}, tim^{L2}, tim^{L1}, tim^{UL}), which suggest that there might be a temperature compensation mechanism

embedded in the system [38, 59]. Moreover, the constraints on the limit cycle hypothesis can be substantially higher and more complicated, if one takes account salinity-compensation and pH-compensation in addition to temperature compensation.

We suggest an alternate hypothesis for robust temperature compensation. Our proposal for temperature compensation imagines that v_p is now a function of time, not a constant parameter. Suppose that v_p is a function of time that starts at an initial value in the region of the stable steady state. Furthermore, suppose that v_p increases exponentially. Then $\frac{dv_p}{dt} = \mu \cdot v_p$, where μ determines how fast v_p increases. As v_p passes through the SNIC bifurcation point at $v_p = 3.28$ (Fig. 2.2.2A), the system enters into the region of unstable steady state with periodic oscillations, which triggers the concentration of PER protein to cycle. When the protein level decreases to a threshold level ($P_t = 2$), v_p is reset by a factor, $\sigma < 1$. In this hypothesis, the period of the oscillation, T, is only dependent on two parameters: μ and σ, and the period of oscillation is insensitive to variations of all other parameters ($T = \frac{1}{\mu} \cdot \ln \frac{1}{\sigma}$).

With v_p as a variable, we can follow the periodic oscillations of mRNA, protein, and v_p (Fig. 2.2.3). v_p increases exponentially, and resets itself by a factor of σ when the total protein concentration passes through the threshold value. Therefore, mRNA and protein oscillate with the period of v_p, which is insensitive to all parameter variations except for μ and σ.

Although v_p (t) is a discontinuous variable, this causes no problem for the numerical integration scheme. Taking PER protein and v_p as function of time from figure 2.2.3, we plot these variables against one another in figure 2.2.2A to obtain the trajectory (— • —). Doing so, we see that the numerical solution of the full set of differential equations is trying to follow the stable solutions of the reduced set of differential equations (where v_p is treated as a constant). For this reason, we can use one parameter bifurcation diagram (v_p = parameter) to understand the dynamics of the more complex control system where v_p is a variable undergoing discontinuous changes at certain time points.

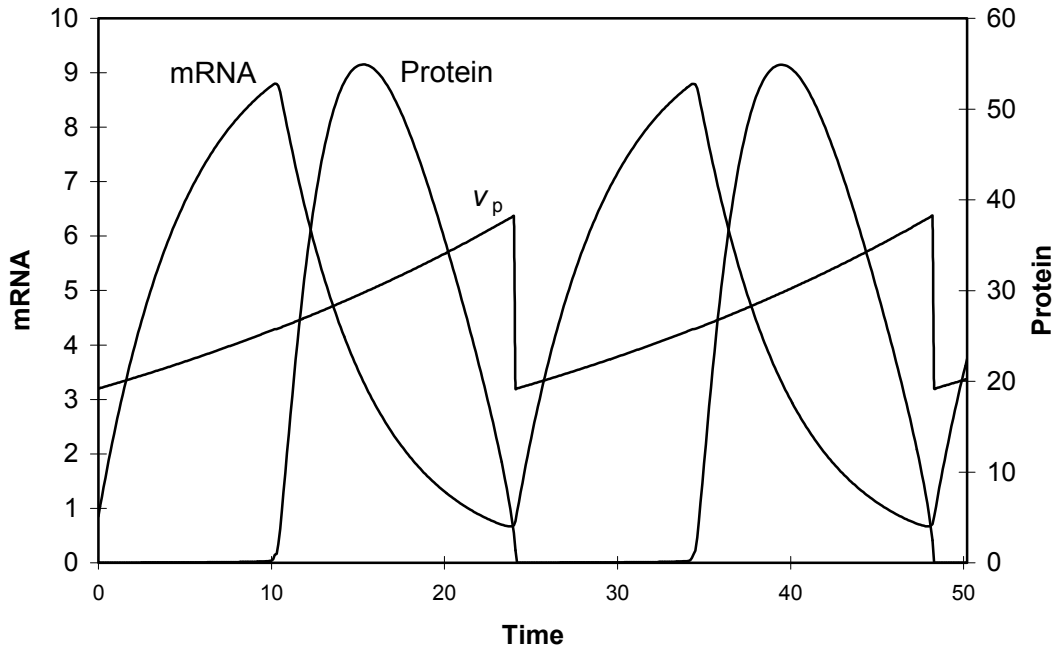

Figure 2.2.3 Time course of *per* mRNA, protein, and v_p

$\mu = 0.0288$ and $\sigma = 0.5$

In order to test the model for robustness of period, we increased and decreased each of the parameters by a factor of two, and then observed any changes of period or stability of the system. As the table 2.2.1 indicates, the period of oscillation is unchanged by all parameter variations except when the rate of mRNA degradation, k_m, is decreased from 0.2 to 0.1. In this particular case, PER concentration never drops below the threshold value, so v_p is never reset. v_p increases to some large value and the control system settles onto a stable steady state. Moreover, we also increased all parameters values except k_m by a factor of two, and still observed a period of about 24 hours (data not shown).

Table 2.2.1 Robust period in parameter variations

Parameter	Default	2x increase	Period	2x decrease	Period
v_m	2	4	24.067	1	24.067
k_m	0.2	0.4	24.067	0.1	s. s. s.
k_{p1}	60	120	24.067	30	24.067
k_{p2}	0.6	1.2	24.067	0.3	24.067
k_{p3}	0.2	0.4	24.067	0.1	24.067
K_{eq}	1	2	24.067	0.5	24.067
P_{crit}	0.6	1.2	24.067	0.3	24.067
J_p	0.05	0.1	24.067	0.025	24.067

A brief pulse of light can shift the phase of free-running rhythms in constant darkness. Phase response curve (PRC) conveniently describes phase differences between the initial phase and the phases after the perturbation. In the experiments, organisms are entrained to 12-hour light and 12-hours dark cycles for several days, and then they are put into constant darkness (t = 0, phase = $\phi_{init} = 0$). A new phase (ϕ_{new}) is created by applying a light pulse (ϕ_{pulse}) at different phases in the cycle, and phase differences are measured relative to initial phase at ($\Delta\phi = \phi_{new} - \phi_{init}$).

In our previous model with limit cycle hypothesis, the light pulse triggered the degradation of protein, which created qualitatively similar PRCs to the experiments (Fig. 2.1.10). For our model with resetting hypothesis, we have discovered that light stimulated degradation of protein alone is not sufficient to generate proper PRCs. This new phase (ϕ_{new}) created by the light pulse is eventually brought back to the old phase (ϕ_{init}) in later cycles (after more than 25 cycles), nullifying both phase advances and delays. The phase of the oscillation created by our resetting hypothesis (v_p exponentially increasing and setting back by a factor of σ) is not able to describe the permanent phase shift based on the degradation of protein level alone upon the pulse of light. The perturbation on protein degradation created initial delays or advances, but the

invariable (or unchanging) translational efficiency (v_p) brought back the new phase to its old phase.

In order for the resetting hypothesis to generate proper PRCs, we must assume that light has two effects on the mechanism: to degrade proteins and to shift the value of v_p. v_p, decreases by light pulse when v_p is in the region of an increasing slope of protein, and increases by light when v_p is in the region of a decreasing slope of the protein. Change of v_p caused permanent phase delays when it was decreased by a light pulse, and permanent phase advances when it was increased by a light pulse. We model these effects as follows:

[Equation 2.2.2] $$\frac{dM}{dt} = v_m \cdot \frac{1}{1+(\frac{P_t \cdot (1-q)}{2 \cdot P_{crit}})^2} - k_m \cdot M$$

[Equation 2.2.3] $$\frac{dP_t}{dt} = v_p \cdot M - \frac{k_{p1} \cdot P_t \cdot q + k_{p2} \cdot P_t}{J_p + P_t} - k_{p3} \cdot P_t - a \cdot pulse(t-\tau) \cdot P_t$$

[Equation 2.2.4] $$\frac{dv_p}{dt} = \mu \cdot v_p + a \cdot pulse(t-\tau) \cdot b \cdot (c_1 - v_p) \cdot (c_2 - v_p) \cdot (c_3 - v_p) \cdot P_t$$

[Equation 2.2.5] $$pulse(t) = heav(t) \cdot heav(pulselength - t)$$

In figure 2.2.4, we show two topological types of PRCs: Type 0 and Type 1. PRCs on the bottom (C and D) are from experimental data [3, 56], and PRCs on the top (A and B) are from our simulations. There is reasonable qualitative agreement between the model and the observations.

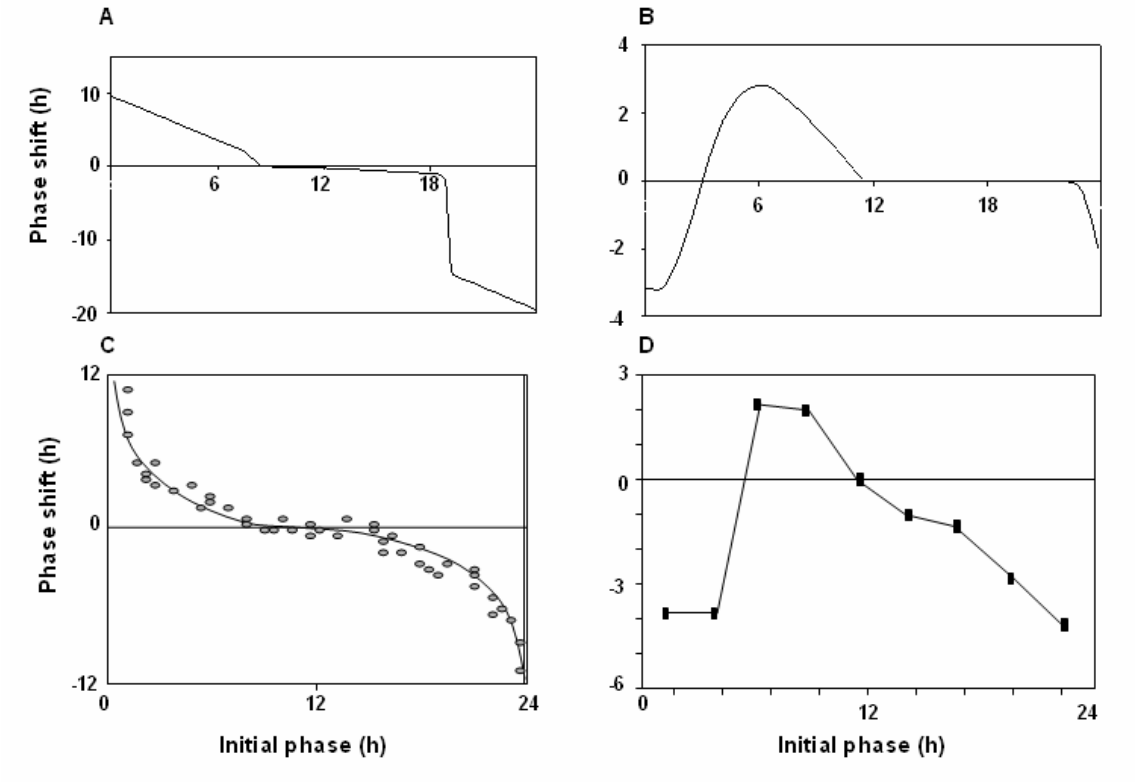

Figure 2.2.4 Phase response curves

For two different types of PRCs, the parameter values are: a=0.1 (Type 1) or a=5 (Type 0), b=1, c_1=2.5, c_2=4.38, c_3=5.8.

It is quite hard to imagine that the translational efficiency (v_p) is the sole foundation of the oscillation. We are not proposing that it is. Rather, we are proposing a possible general idea, which could be applied to a circadian rhythm mechanism containing both positive and negative feedback loops. Our proposed mechanism for oscillations is generic in the sense that it does not rely on specific assumptions about mechanisms or parameter values. We only require that the mechanism show a bifurcation structure for some components that might undergo a process of steady increase followed by periodic resetting. In the next chapter, we will continue with our comprehensive model, which has 12 equations and 32 parameters, and show that this idea can be further pursued in the basis of bifurcation analysis and experimental facts.

Chapter 3 Comprehensive Model

3.1 Realistic Model and Equations

A more realistic model is derived by relaxing most of the assumptions from our simple model. PER and TIM proteins are synthesized from transcription factors, dCLK and CYC. Monomer forms of PER proteins are susceptible for phosphorylation by DBT and therefore degraded, whereas the dimer forms or complexes with TIM are stable. PER and TIM complexes are translocated into the nucleus, and nuclear PER forms an inactive complex with transcription factors dCLK and CYC, and thereby inhibits its own transcriptions. In addition, there is indirect negative feedback on the transcription of *dClk*, by transcription factors. This feedback is actually mediated by VRILLE (VRI) protein. VRI is activated by dCLK, but enters into the nucleus and inhibits the transcription of *dClk*. In our model, we describe this as a direct inhibition by dCLK for simplicity of the model. This model is described as in figure 3.1.1. This model is converted into 12 differential equations (Table 3.1.1) with 32 parameters (Table 3.1.2), and simulated for robust oscillations.

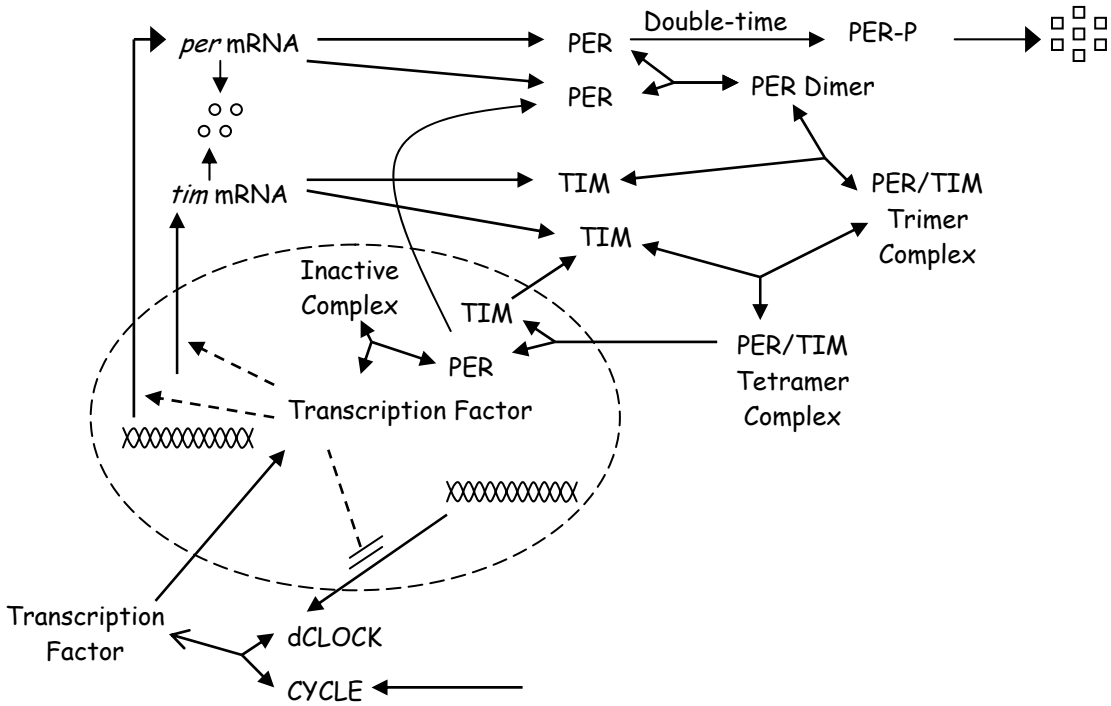

Figure 3.1.1 Schematic model of comprehensive model

Table 3.1.1 Kinetic equations comprehensive model

a) mRNAs of *per*, *tim*, and *dClk*
$\frac{dP_m}{dt} = v_{mp} \cdot \frac{F^m}{K_1^m + F^m} - k_{dmp} \cdot P_m$ $\frac{dT_m}{dt} = v_{mtb} + v_{mt} \cdot \frac{F^m}{K_2^m + F^m} - k_{dmt} \cdot T_m$ $\frac{dC_m}{dt} = v_{mc} \cdot \frac{1}{1 + k \cdot F^n} - k_{dmc} \cdot C_m$

b) PER monomer, homodimer, and nuclear PER

$$\frac{dP_1}{dt} = v_p \cdot P_m - k_{p3} \cdot P_1 - \frac{k_{p1} \cdot P_1}{J_p + P_{tot}} + 2k_{p3} \cdot P_2 + 2k_{p3} \cdot P_2T_1 + \frac{2k_{p2} \cdot P_2}{J_p + P_{tot}} +$$

$$\frac{2k_{p2} \cdot P_2T_1}{J_p + P_{tot}} + \frac{2k_{p2} \cdot P_2T_2}{J_p + P_{tot}} - 2k_{app} \cdot P_1^2 + 2k_{dpp} \cdot P_2 + 2k_{p3} \cdot P_2T_2 + k_{out} \cdot P_N$$

$$\frac{dP_2}{dt} = k_{app} \cdot P_1^2 - k_{dpp} \cdot P_2 - 2k_{p3} \cdot P_2 - \frac{2k_{p2} \cdot P_2}{J_p + P_{tot}} - 2k_{apt} \cdot P_2 \cdot T_1 + k_{dpt} \cdot P_2T_1 + k_{t3} \cdot P_2T_1$$

$$\frac{dP_N}{dt} = 2k_{in} \cdot P_2T_2 - k_{out} \cdot P_N - k_{aitf} \cdot F \cdot P_N + k_{ditf} \cdot F_{inac} + k_{dc}F_{inac} - k_{p3} \cdot P_N - \frac{k_{p1} \cdot P_N}{J_p + P_{tot}}$$

c) TIM monomer

$$\frac{dT_1}{dt} = v_t \cdot T_m - k_{t3} \cdot T_1 + 2k_{p3} \cdot P_2T_1 + \frac{2k_{p2} \cdot P_2T_1}{J_p + P_{tot}} + \frac{4k_{p2} \cdot P_2T_2}{J_p + P_{tot}} + 2k_{apt} \cdot P_2 \cdot T_1 + k_{dpt} \cdot P_2T_1$$

$$-k_{apt} \cdot P_2T_1 \cdot T_1 + 2k_{dpt} \cdot P_2T_2 + 4k_{p3} \cdot P_2T_2 + 2k_{in} \cdot P_2T_2$$

d) dCLK monomer

$$\frac{dC}{dt} = v_c \cdot C_m - k_{dC} \cdot C - k_{acc} \cdot C \cdot Y + k_{dcc} \cdot F$$

e) Complex: PER/TIM trimer, PER/TIM tetramer, transcription factor (dCLK and CYC), and inactive transcription factor (dCLK, CYC, and nuclear PER)

$$\frac{dP_2T_1}{dt} = 2k_{apt} \cdot P_2 \cdot T_1 - k_{dpt} \cdot P_2T_1 - k_{t3} \cdot P_2T_1 - 2k_{p3} \cdot P_2T_1 - \frac{2k_{p2} \cdot P_2T_1}{J_p + P_{tot}} - k_{apt} \cdot P_2T_1 \cdot T_1 + 2k_{dpt} \cdot P_2T_2 + 2k_{t3} \cdot P_2T_2$$

$$\frac{dP_2T_2}{dt} = k_{apt} \cdot P_2T_1 \cdot T_1 - 2k_{dpt} \cdot P_2T_2 - 2k_{t3} \cdot P_2T_2 - 2k_{p3} \cdot P_2T_2 - \frac{2k_{p2} \cdot P_2T_2}{J_p + P_{tot}} - k_{in} \cdot P_2T_2$$

$$\frac{dF}{dt} = k_{acc} \cdot C \cdot Y - k_{dcc} \cdot F - k_{aitf} \cdot F \cdot P_N + k_{ditf} \cdot F_{inac} - k_{dc}F + k_{p3} \cdot F_{inac} + \frac{k_{p2} \cdot F_{inac}}{J_p + P_{tot}}$$

$$\frac{dF_{inac}}{dt} = k_{aitf} \cdot F \cdot P_N - k_{ditf} \cdot F_{inac} - k_{p3} \cdot F_{inac} - k_{dc} \cdot F_{inac} - \frac{k_{p2} \cdot F_{inac}}{J_p + P_{tot}}$$

f) Total Concentration

$$P_{tot} = P_1 + 2P_2 + 2P_2T_1 + 2P_2T_2 + F_{inac}$$

$$T_{tot} = T_1 + P_2T_1 + 2P_2T_2$$

$$C_{tot} = C + F + F_{inac}$$

$$Y_{tot} = Y + F + F_{inac}$$

Table 3.1.2 Basal parameter set of comprehensive model

Name	Value	Description
v_{mp}	1	Maximum rate of synthesis of *per* mRNA
v_{mt}	0	Maximum rate of synthesis of *tim* mRNA
v_{mtb}	1	Background rate of synthesis of *tim* mRNA
v_{mc}	0.025	Maximum rate of synthesis of *dClk* mRNA
k_{dmp}	0.1	First-order rate constant for *per* mRNA degradation
k_{dmt}	0.1	First-order rate constant for *tim* mRNA degradation
k_{dmc}	0.1	First-order rate constant for *dClk* mRNA degradation
v_p	0.5	Rate constant for translation of *per* mRNA
v_t	0.5	Rate constant for translation of *tim* mRNA
v_c	0.5	Rate constant for translation of *dClk* mRNA
k_{p1}	10	V_{max} for monomeric PER phosphorylation
k_{p2}	0.03	V_{max} for dimeric PER phosphorylation
k_{p3}	0.1	First-order rate constant for proteolysis of PER
k_{t3}	0.1	First-order rate constant for proteolysis of TIM
k_{dc}	0.1	First-order rate constant for proteolysis of dCLK
k_{app}	10	Association rate const for PER-PER homodimerization
k_{dpp}	0.1	Dissociation rate const for PER-PER homodimerization
k_{apt}	10	Association rate const for PER-TIM heterodimerization
k_{dpt}	0.1	Dissociation rate const for PER-PER heterodimerization
k_{acc}	10	Association rate const for CYC-dCLK heterodimerization
k_{dcc}	0.1	Dissociation rate const for PER-PER heterodimerization
k_{aitf}	10	Association rate const for PER-F for complex formation
k_{ditf}	0.1	Dissociation rate const for PER-F for complex formation
k_{in}	1	Nuclear transport rate constant
k_{out}	0.1	Nuclear export rate constant
K_1	1	Michaelis constant for synthesis of *per* mRNA
K_2	1	Michaelis constant for synthesis of *tim* mRNA
m	7	Hill exponent of *per* and *tim* mRNA synthesis

n	2	Hill exponent of *dclk* mRNA synthesis
Y_{tot}	10	Total concentration of CYCLE protein
J_p	0.05	Michaelis constant for protein kinase (DBT)
k	0	A constant for the activity of dCLK feedback loop

3.2 Bifurcation Analysis

There are three feedback loops intertwined with each other in our comprehensive model (Fig. 3.1.1): 1) a negative feedback loop inhibiting both *per* and *tim* transcriptions by PER, 2) another negative feedback loop on transcription of *dClk*, and 3) a positive feedback loop based on the stabilization of PER upon dimerization. It is not trivial to understand the dynamics of the interactions of these three loops. Therefore, we want to start with similar dynamics as in our simple model: active loops on PER negative and positive feedbacks, but inactive feedbacks on both TIM and dCLK. In this way, we can find a parameter space where we desire to be, and expect qualitatively similar dynamics as in our simple model. We set parameters k and v_{mt} to zero, which inactivates transcriptional feedbacks on both *dClk* and *tim*. And we set the background rate of synthesis of *tim* ($v_{mtb} = 1$) for constant synthesis of TIM.

In order to demonstrate that our intuition is indeed correct, we generate qualitatively similar bifurcation pictures as in figures 2.1.12. We follow the steady state level of total PER protein in function of phosphorylation induced degradation rate of monomeric PER proteins, k_{p1}. As we expected, we observe hysteresis induced by the autocatalysis of PER, and a Hopf bifurcation contributed from the negative feedback loop from PER dynamics (Fig. 3.2.1). The basal parameter set from table 3.1.2 is used for the analysis. As we further follow these bifurcation points in two parameters, k_{app} (comparable to K_{eq}) and k_{p1}, we show a similar diagram as in 2.1.13 (Fig. 3.2.2). Hopf bifurcation ends in tangent with saddle-node (SN) bifurcation [57]. Also, saddle-node bifurcations with a region of multiple steady states with cusp are shown [57].

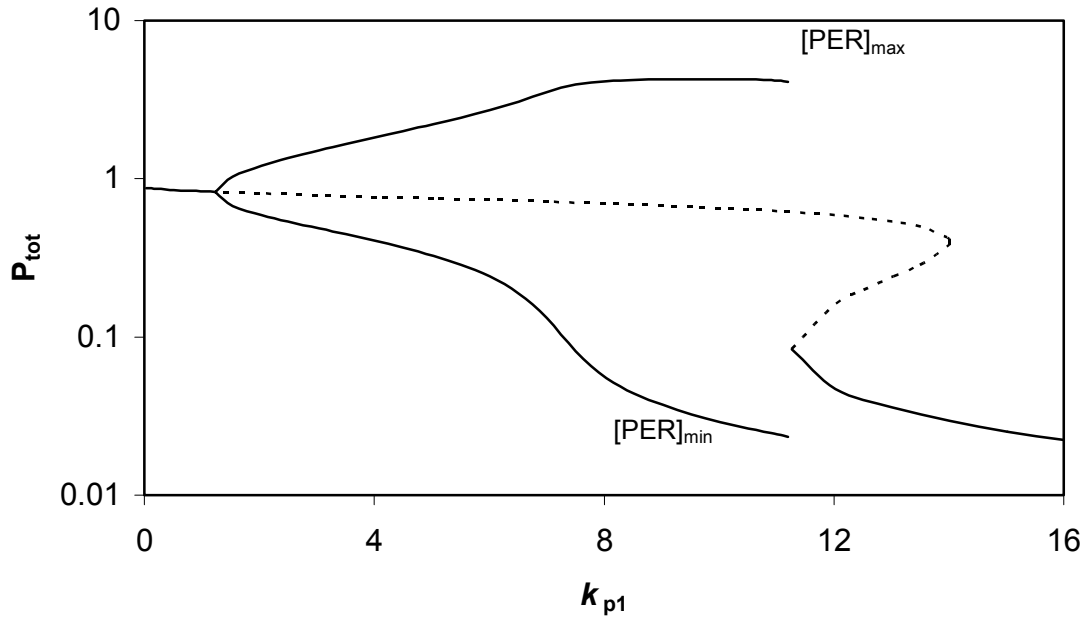

Figure 3.2.1 One parameter bifurcation diagram with k_{p1}

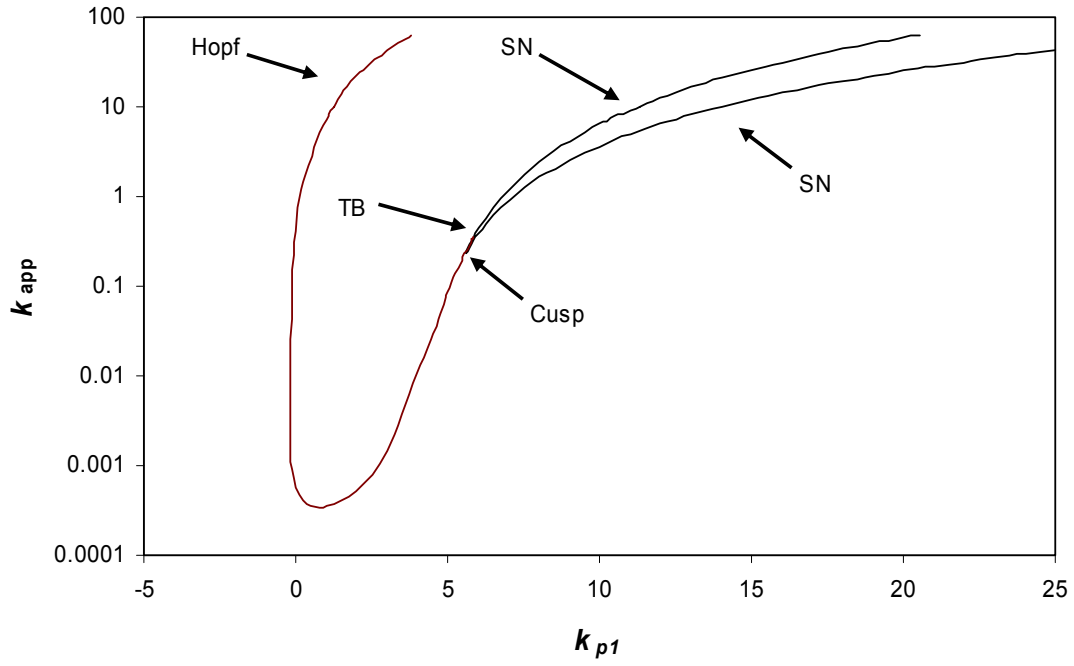

Figure 3.2.2 Two parameter bifurcation diagram: k_{app} vs. k_{p1}

Hysteresis is also observed when we plot the one-parameter bifurcation diagram in dependence on v_{mc}, rate of *dClk* translation (Fig. 3.2.3). As with k_{p1}, hysteresis and Hopf bifurcations are noted. However, we observe two Hopf bifurcations instead of one as in figure 3.2.1. We further followed this in two-parameter space, k_{p1} and v_{mc} (Fig. 3.2.4), in order to find out the dynamical changes in relation to variations in both the monomeric degradation rate (k_{p1}) and the transcription rate of *dClk* (v_{mc}). There is a region of multiple steady states within SN bifurcations with cusp. Both Hopf bifurcations end in tangent at codimension two Takens-Bagdanov bifurcation points.

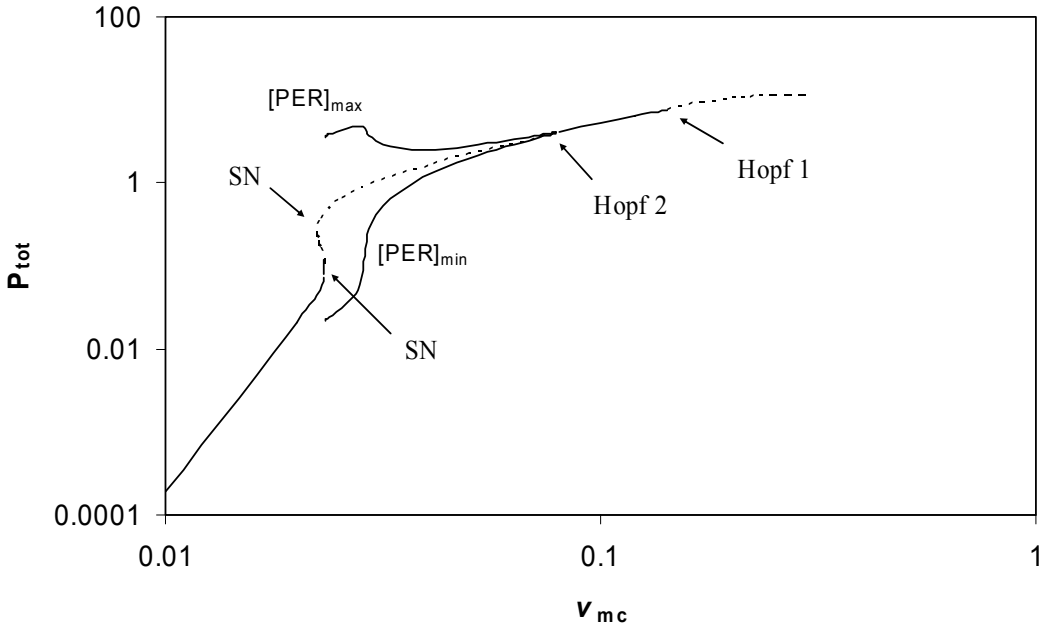

Figure 3.2.3 One-parameter bifurcation diagram with v_{mc}

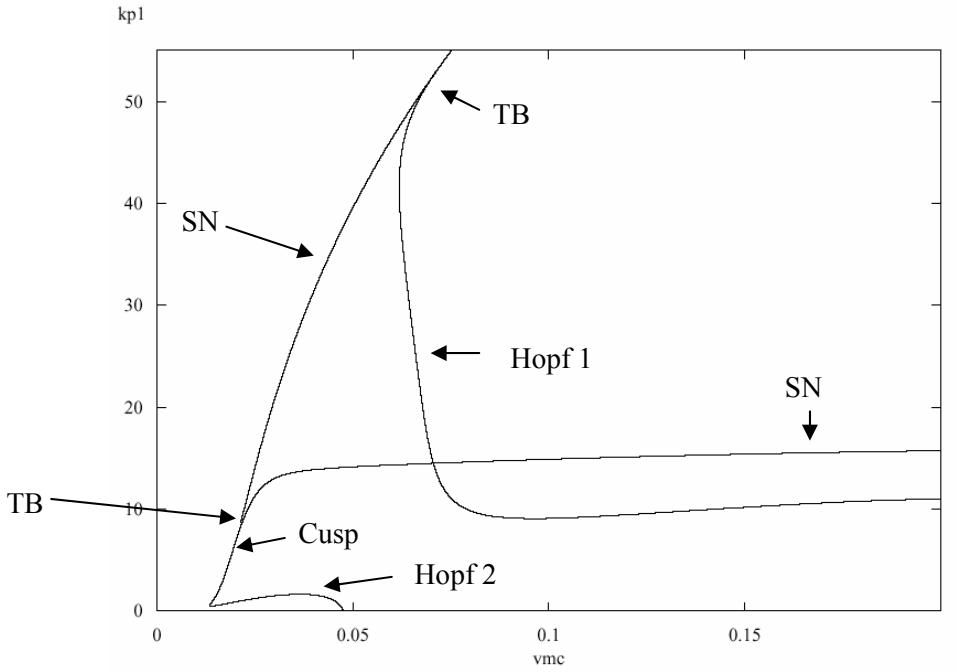

Figure 3.2.4 Two-parameter bifurcation diagram: k_{p1} vs. v_{mc}

Our next task is to determine the dynamics involved with nuclear entry, because nuclear translocation plays such an important role in the system of circadian rhythms. With a set of parameter values that we used for previous analysis (Table. 3.1.2), we followed the steady state level of total PER in the function of the nuclear transport rate, k_{in} (Fig. 3.2.5A). As before, we find hysteresis and large amplitude oscillations. The period of the system increases as the nuclear transport rate (k_{in}) increases (Fig. 3.2.5B). However, the period seems to be quite insensitive for large region of k_{in} ($0.2 < k_{in} < 2$), and then increases to infinite period as the system gets closer to SNIC bifurcation.

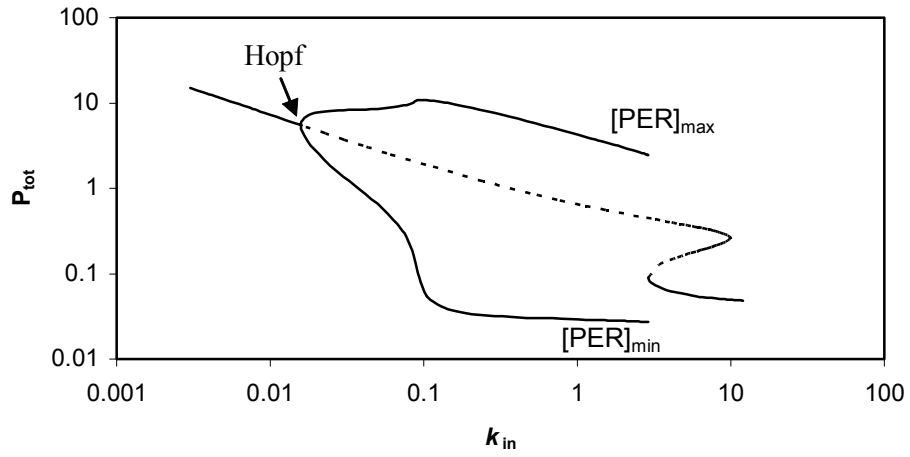

Figure 3.2.5A One parameter bifurcation diagram of k_{in} with feedbacks on *tim* and *dClk* OFF

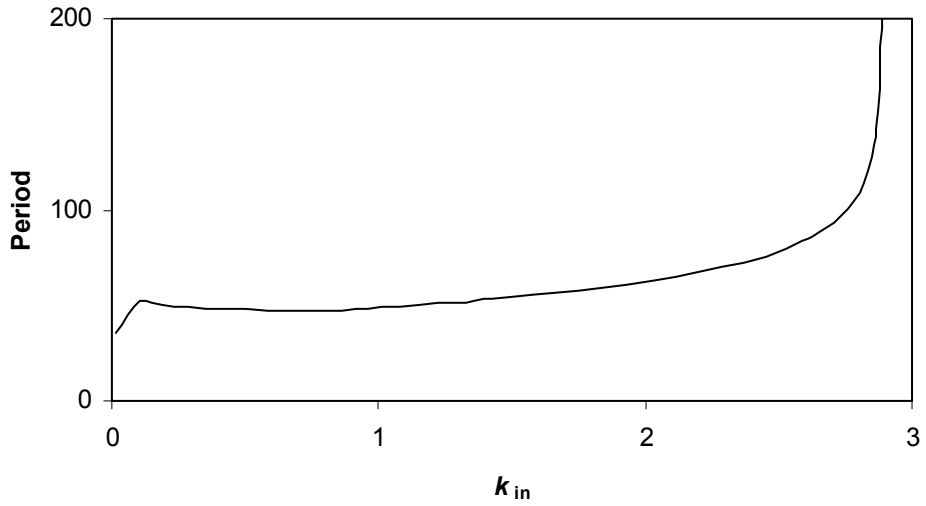

Figure 3.2.5B Period dependency on k_{in}

In an attempt to verify the role of the positive feedback loop in the system, we knocked out the autocatalysis by making the monomers as stable as dimers ($k_{p1} = k_{p2} = 0.03$). As shown in figure 3.2.6, hysteresis disappears, and a stable limit cycle is created by Hopf bifurcation from time-delayed negative feedback loop alone.

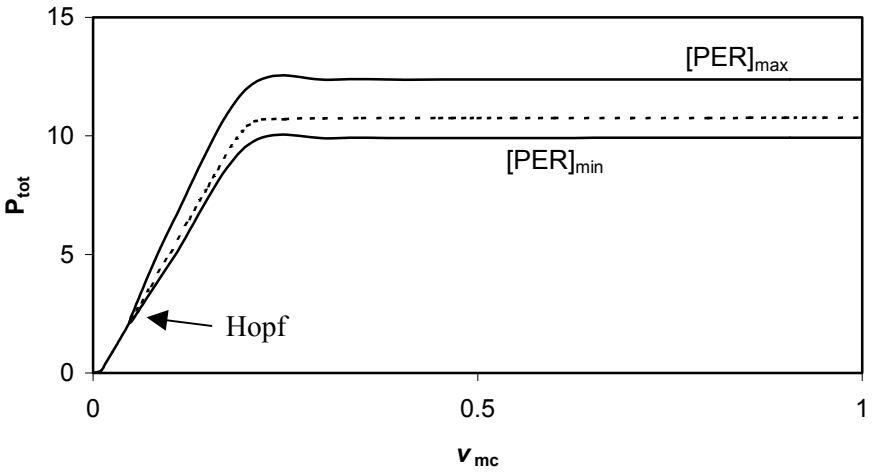

Figure 3.2.6 One parameter bifurcation diagram of v_{mc} with $k_{p1} = 0.03$

Now that we have shown that our comprehensive model has qualitatively similar dynamics as our simple model, we took the next step, which is to activate other feedbacks in the system. First of all, we turned on negative feedback on *tim* transcription ($v_{mt} = 1$ and $v_{mtb} = 0$), and calculated the two parameter bifurcation diagram for k_{p1} vs. v_{mc} as in figure 3.2.4. Bifurcation analysis shows very similar dynamics (Fig. 3.2.7). This is what we expected, because the dynamics of TIM largely depends on PER. It is PER that drives both negative feedbacks on PER and TIM thereby creating similar phases of their cycles. As long as TIM is not a limiting factor hindering the nuclear transport of PER, oscillation will persist without disruption.

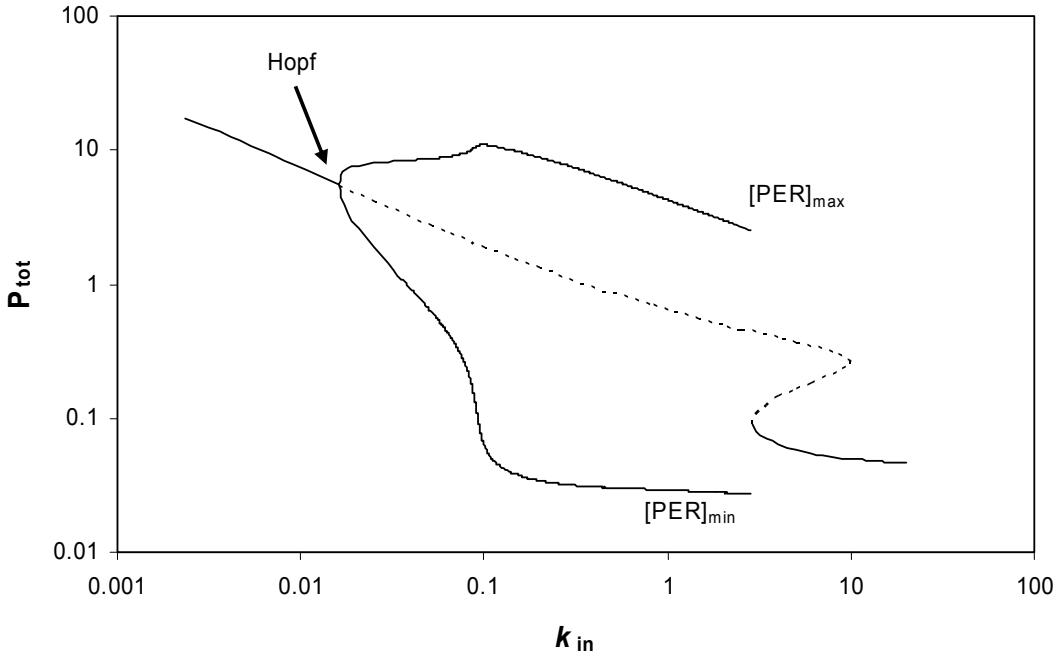

Figure 3.2.7 One parameter bifurcation diagram of k_{in} with negative feedback on *tim* transcription (v_{mt}=1, v_{mtb}=0)

Next we activate another negative feedback loop on *dClk* transcription by setting the strength of the feedback (k) from 0 to 0.1. The realistic model with all the feedbacks ON, displays qualitatively similar bifurcation diagram to our previous analysis: Hopf and SNIC bifurcations with large amplitude oscillation, and hysteresis (Fig. 3.2.8).

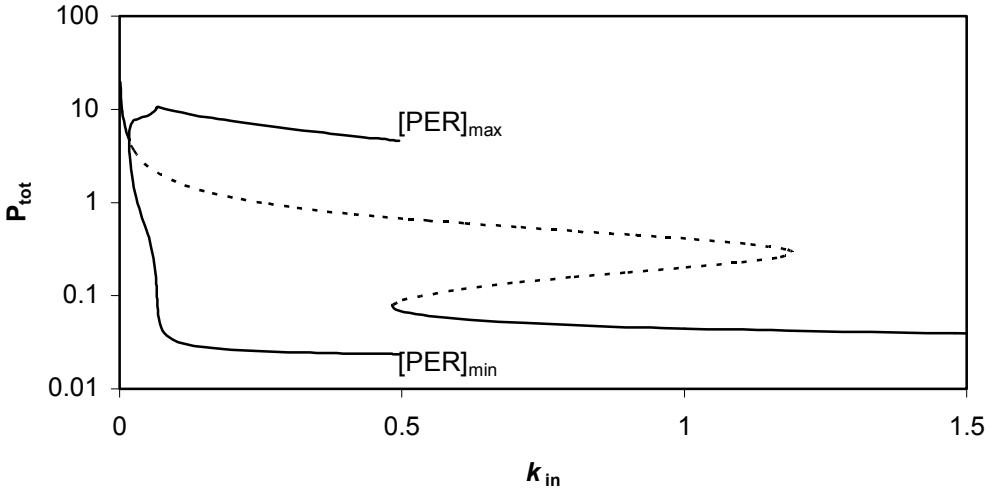

Figure 3.2.8 One parameter bifurcation diagram of k_{in} with all the feedbacks ON
Parameter values are as in figure 3.2.1 except: v_{mt}=1, v_{mtb}=0, k=0.1

The overall bifurcation analysis indicates the consistent dynamical behavior from our simple model with both autocatalysis and negative feedback loop (Hopf and SNIC bifurcations with large amplitude oscillation, and hysteresis) is retained even in the realistic model with multiple feedback loops. Although it is not intuitive how the system will behave upon additions of other feedback loops (negative feedback loops on *tim* and *dClk* transcriptions), bifurcation analysis clearly depicts the core dynamics based on the autocatalysis and negative feedback loop. Moreover, analysis specifically indicates a role of positive feedback loop based on the stabilization of PER protein (Fig. 3.2.6). In Chapter 4, I will use our analysis to suggest possible experimental hypotheses to be tested.

3.3 Revisiting the Resetting Hypothesis

The bifurcation analysis in section 3.2 describes only a small portion of the entire parameter set in our comprehensive model. The enriched dynamics generated by both positive and negative feedbacks suggest that the control system of circadian rhythms can exhibit dynamical behavior much richer than a simple limit cycle oscillator. We could apply our resetting hypothesis from the simple model to the realistic model. We now have several candidates of parameters (i.e. k_{in}, v_{mc}, etc.) that show hysteresis with both SNIC and Hopf bifurcations.

Among the choices that we have, the most plausible idea is the variable activity of nuclear translocation. How? We might imagine that some necessary component for translocation of PER-TIM complexes into the nucleus loses activity exponentially, or perhaps by degradation or disassembly. Then, when PER proteins are degraded, the translocation machinery is reactivated, perhaps by a template-directed reconstruction of active pore components. Yet another scenario can be imagined. Assume that the nuclear transport rate is the function of multiply phosphorylated forms of PER or TIM (that progressive phosphorylation of PER or TIM with a large number of cooperativity is required for nuclear localization). Then, this PER and TIM will accumulate in the cytoplasm being unable to enter into the nucleus until multiple phosphorylation is satisfied. Once the multiple phosphorylation requirement is satisfied, they enter into the nucleus, and the nuclear transport rate is reset as PER and TIM are degraded in the nucleus while inhibiting their own synthesis. In either cases, they will create a gated transport of PER and TIM proteins, which could be seen from an unpublished video clip of nuclear translocation of PER and TIM proteins. [Michael Young, private communication]

In order to generate robust rhythms of about 24 h, I revised some of the parameter values in Table 3.1.2 and computed a one parameter bifurcation diagram for k_{in} (Fig. 3.3.1). Qualitatively similar dynamical properties exist between figures 3.2.5A and 3.3.1. Our resetting hypothesis can be applied as in our simple model. k_{in} decreases exponentially (half-life = 6.9 h or $\mu = 0.1$) and when it crosses the SNIC bifurcation point, the system enters into the region of stable limit cycle. When PER protein level

decreases to the threshold level (P_{thres} = 1), k_{in} increases abruptly by a factor σ = 11. As expected ($T = \frac{1}{\mu} \cdot \ln \sigma$), the resetting mechanism generates a robust oscillation with a period of 24 h, which is insensitive to most parameter values in the system. The oscillation path is denoted by (— • —) in figure 3.3.1.

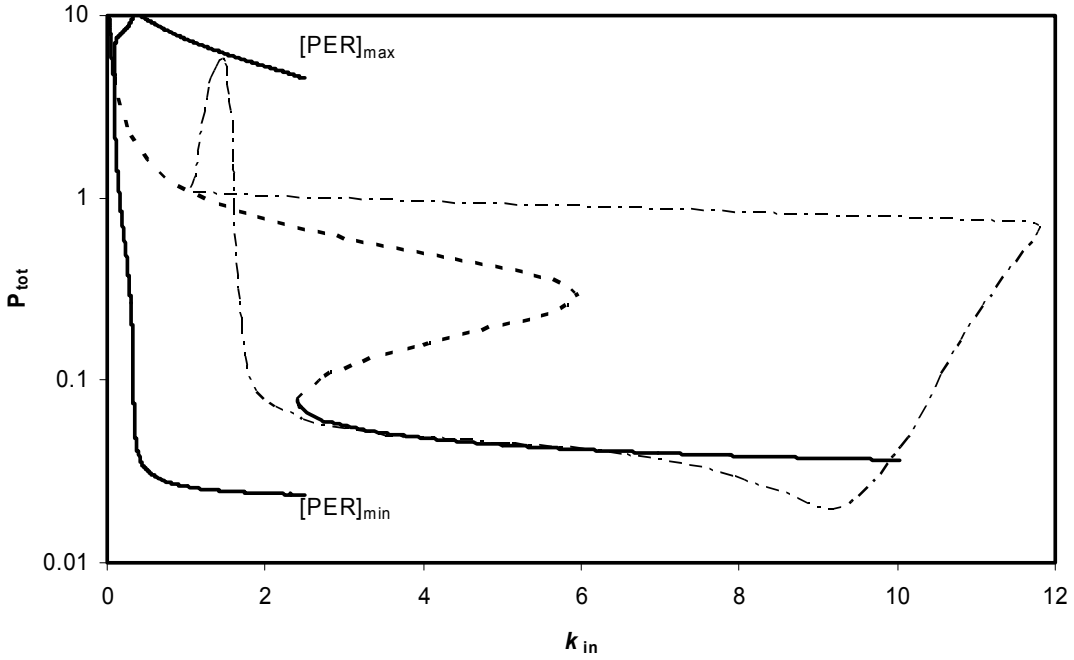

Figure 3.3.1 One parameter bifurcation diagram of k_{in}

Parameter values are as the following: v_{mp}=5, v_{mt}=5, v_{mc}=0.125, k_{dmp}=0.5, k_{dmt}=0.5, k_{dmc}=0.5, v_p=2.5, v_t=2.5, v_c=2.5, k_{p1}=50, k_{p2}=0.15, k_{p3}=0.5, k_{t3}=0.5, k_{dc}=0.5, k_{app}=50, k_{dpp}=0.5, k_{apt}=50, k_{dpt}=0.5, k_{acc}=50, k_{dcc}=0.5, k_{aitf}=50, k_{ditf}=0.5, k_{in}=5, k_{out}=0.5, K_1=1, K_2=1, m=7, n=2, Y_{tot}=10, J_p=0.05, k=0.1

Several mutations are known to change the period of endogenous circadian rhythms. Within the "resetting" hypothesis context, such mutation must interfere with μ and/or σ. Mutations might destroy the SNIC bifurcation and force the central system into the limit cycle mode. Such mutations may retain the property of temperature compensation or they may lose temperature compensation, and the system becomes sensitive to temperature changes. More exploration of the model and concurrent

experiments will aid in understanding and identifying a possible mechanism of temperature compensation. In our next chapter, we will discuss how to apply and test our hypothesis in *Neurospora crassa* circadian rhythms.

Chapter 4 Conclusion and Future Prospectus

4.1 Brief Summary

The molecular findings of core components of circadian rhythms in *Drosophila melanogaster* provided us with enough data to build a plausible model of the biological clock mechanism. About a dozen components were used to make a wiring diagram of this control system (Fig. 3.1.1). The wiring diagram is converted into a set of 12 ordinary differential equations with 32 parameter values. Then, the model is simulated and analyzed by using a numerical analysis software XPPAUTO.

Our analysis of the comprehensive model indicates that it simulates observed physiological properties of circadian rhythms (free-running endogenous rhythms, phase shift by light, and temperature compensation). Moreover, our analysis gives an insight of different functions played by each of feedback loops present in the control system. The time-delayed negative feedback of PER protein creates a Hopf bifurcation with an oscillatory domain. The autocatalysis based on PER protein proteolysis and stabilization generates hysteresis, with a region of multiple steady states. Other negative feedback loops on TIM and dCLK dynamics are not required for the oscillation of the system. TIM dynamics follow the behavior of PER proteins due to the fact that PER regulates *tim* mRNA transcriptions. Even though the negative feedback loop on dCLK is not necessary for the oscillation of the system, this feedback mechanism may be involved in generating the output from the core mechanism [60-62].

In conclusion, the mechanism of circadian rhythms in *Drosophila melanogaster* is controlled by a complex molecular mechanism consisting of both positive and negative feedback loops. Previous models adopted a limit cycle hypothesis in order to explain the basic properties of circadian rhythms. Even though the limit cycle hypothesis satisfies three out of four properties of circadian rhythms, it faces a major problem when it comes to explain robust temperature compensation of the endogenous rhythm. We propose the existence of autocatalytic effect of PER protein accumulation based on the dynamics of PER and DBT. Furthermore, we propose a robust mechanism for temperature compensation based on parameter resetting across a SNIC bifurcation in

the presence of both positive and negative feedback loops. The resetting hypothesis is generic because SNIC bifurcations are commonly observed in nonlinear control systems with both positive and negative feedback loops. This idea will be pursued experimentally at Dartmouth Medical School, and experimental evidence for molecular candidates for the resetting hypothesis will be sought.

4.2 Future Directions

4.2.1 Further Modeling

The modeling of circadian rhythms in *Drosophila melanogaster* needs further development in order to accurately account for observed phenotypes. From the components that we have discussed, but not included in our comprehensive model are CRY, PDP1 and VRI. A photoreceptor protein, CRY, needs to be incorporated into the model in order to describe detail interactions with TIM and subsequent degradation of TIM upon a light pulse. This may be helpful in simulating better phase response curves in comparison to experimental data.

PDP1 and VRI constitute feedback loops involved with transcription factors, dCLK and CYC. Positive effect of PDP1 and negative effect of VRI on *dClk* mRNA transcriptions may generate another biochemical oscillator separate from the core oscillator based on positive and negative feedback loops driven by PER protein dynamics. The core oscillator driven by PER protein dynamics may be coupled to another oscillator in order to generate robust output signals. Even though the current knowledge of PDP1 and VRI indicates their positive and negative roles on *dClk* mRNA transcriptions, there are still missing pieces of the puzzle in order to create a robust oscillator apart form PER protein dynamics. Maybe there exists a long time-delay between the expression of VRI and its inhibition on *dClk* mRNA transcription, which creates a stable limit cycle oscillation. It would be a worthwhile project to find out how a core oscillator based on resetting hypothesis interacts with another oscillator based on time-delayed negative feedback loop in generating outputs of circadian rhythms.

4.2.2 Circadian Rhythms in *Neurospora crassa*

The molecular network regulating the circadian rhythms in *Neurospora crassa* is quite similar to *Drosophila melanogaster*. Homologous components between fruit flies and bread molds are described in Table 4.2.1. FREQUENCY (FRQ) seems to be a core component (PER in *Drosophila*). Heterodimer, WHITE-COLLAR-COMPLEX (WCC, comparable to dCLK-CYC heterodimer), act as a positive element to drive the synthesis of negative element, FRQ [63, 64]. FRQ translocates into the nucleus for self-inhibition by binding to WCC [65]. It has been shown that FRQ gets progressively phosphorylated by casein kinase, CKII, and then degraded [66, 67]. FRQ forms homodimers by coiled-coil domain interactions, but it has not been established whether there exist stability differences between monomeric FRQ vs. FRQ homodimers [68].

From modeler's perspective, our simple model can be applied to illustrate the dynamics of bread mold's biological clocks (Fig. 4.2.1). Due to the fact that FRQ forms homodimers instead of heterodimers as in fruit fly, it is even more suitable to apply our simple model to bread molds than fruit flies. Figure 4.2.1 describes identical dynamics as in our simple model: the autocatalysis of FRQ proteins based on its proteolysis and degradation, and the negative feedback of *frq* mRNA by FRQ proteins.

Table 4.2.1 Homologous components between *Drosophila melanogaster* and *Neurospora crassa*

Drosophila	Properties	*Neurospora*
per	Physically binds to transcription factors. Inhibit its own transcriptions.	*Frq*
dClk	Cycles with circadian rhythm. Binds with its partner to form a transcription factor and induces transcriptions of circadian rhythms components.	*wc-1*
cyc	Constitutively expressed. Binds with its partner to form a transcription factor and induce the transcriptions of circadian rhythms components.	*wc-2*
dbt	Kinase which phosphorylates PER or FRQ and triggers proteolysis of each protein.	*ckII*

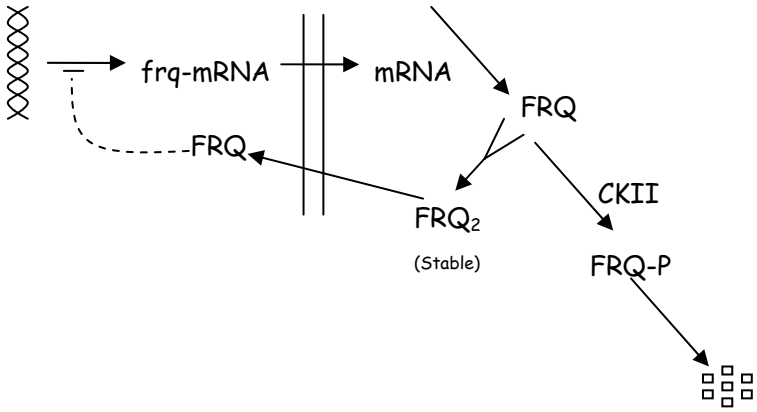

Figure 4.2.1 Schematic model of *Neurospora* clock mechanism

As our first hypothesis to be tested, we propose to test for the existence of hysteresis in the system. This switch-like behavior will be indicated as a critical level or threshold of FRQ concentration required for its abrupt increase induced by the

autocatalysis. Based on evidences in *Drosophila melanogaster* circadian rhythms components, we speculate the stability differences between monomers and dimers of FRQ underlie the foundation of positive feedback loop in the system. Therefore, we propose to study the detailed proteolysis of FRQ in its different forms. Nuclear transport of FRQ is an essential dynamics for circadian rhythms in *Neurospora crassa*. Experimentally, it has been shown that a deletion of nuclear localization signal (NLS) domain yields stable FRQ, which is blocked for nuclear transport. We also need to clarify how NLS contributes to the stability of FRQ.

Our model suggests an oscillator driven by an irreversible switch, and is insensitive to most of the parameter variations. In this way, the property of temperature compensation is embedded in the wiring diagram of the system, and not presented as means of balancing all the kinetic parameters in effect of temperature. We hypothesize a possible mechanism for temperature compensation, and we suggest screening for strains bearing mutations in temperature compensation mechanism. Close collaboration of experiments and modeling will be used in attacking the problems and resolving each one of them. Possible synergy of experiments and modeling of circadian rhythms in *Neurospora crassa* will yield better understanding of the dynamical processes involved in the system.

4.3 Hypotheses to Be Tested

In January 2004, I plan to begin a postdoctoral research program at Dartmouth Medical School, under the guidance of Dr. Jay Dunlap, in order to test several hypotheses generated by this dissertation work. I hope to obtain experimental evidence relevant to the mechanism of robust temperature compensation of circadian rhythms. Although we are proposing the presence of an autocatalysis based on self-stabilization of FRQ, it could be revealed that this effect is not relevant. Nevertheless, hypotheses below are about crucial dynamical processes in the system, which will reflect important functions of dimerization, phosphorylation, nuclear transport, and temperature compensation mechanism. The results from these tests will provide information to improve the model. A close interaction between experimental studies and computational modeling will provide a firm foundation for understanding the core mechanism of circadian rhythms.

In collaboration with Dr. Dunlap, I have designed the following specific hypotheses to be tested:

- Aim 1: to verify the existence of hysteresis in the system.

In order to test our hypothesis, we need to knockout the negative feedback loop and to artificially control the production of FRQ. In a knock out mutant, we would expect to see either a high steady state or a low steady state with hysteresis generated by a positive feedback. In the absence of a negative feedback loop, the upper unstable steady state with stable limit cycle would disappear (Fig. 2.2.2), and be substituted with high stable steady state. By controlling the synthesis of FRQ in entirely heterologous promoter (QA2 promoter) in frq^0 mutant, I should be able to determine the critical level of FRQ where the autocatalysis becomes active and results in an abrupt increase of FRQ level.

- Aim 2: to test for detailed function of coiled-coil dimerization and stabilization of FRQ by dimerization.

I will experimentally test the role of the coiled-coil domain in determining the stability of FRQ. Using an Myc epitope-tagged version of FRQ, Cheng et. al. [68] have

deleted the coiled-coil domain and also generated several point mutants that decrease the interaction among FRQ monomers. These strains and constructs are in hand, and I will engineer a strain in which the mutant FRQ can be induced by quinic acid. By transforming these mutant genes into a strain with a HA-tagged wild type copy of FRQ, I will be able to examine and compare the half-lives of monomer versus dimerized FRQ in these strains. Briefly, under conditions where the clock is running normally in the dark, I will add the inducer (quinic acid) which will result in rapid expression of FRQ to wild type levels within 2 hours[59,60]. At this point I will wash away the inducer and remove samples every hour for 6 hours. Following extraction of cellular proteins, dimerized FRQ will be determined by immunoprecipitation with anti-HA followed by western blotting with anti Myc. From the immunoprecipitation supernate, monomeric FRQ can be collected by immunoprecipitation with anti-Myc. In this way I will be able to follow the entry of FRQ into dimers as a function of the different point mutations and the stability of monomeric versus dimeric FRQ.

- Aim 3: to verify the significance of the nuclear localization signal and will look to see whether there is different stability of FRQ in the cytoplasm vs. the nucleus.

Nuclear localization of FRQ protein is essential for clock to function. A deletion of nuclear localization signal (ΔNLS) domain in *frq* gene results in a block to nuclear transport of FRQ [65]. In addition, deletion of NLS creates a stable FRQ that displays no fluctuations in its phosphorylation levels. However, the CKII binding site of FRQ is located close to the NLS domain, so it is possible that the ΔNLS construction disrupted a kinase-binding FRQ, and thereby creating stable, hypophosphorylated FRQ proteins [64]. Therefore, it is important to sort out the role of nuclear localization in the stability of FRQ, and the role of sequences near to the NLS in FRQ phosphorylation.

I will first determine using phosphopeptide mapping whether the potential phosphorylation site near to the NLS is normally phosphorylated in vivo and ether this is affected in the ΔNLS strain. If it is affected, I will by trial and error re-engineer point mutations within the NLS to destroy its function without affecting surrounding regions, in particular the phosphorylation site. Since the FRQ NLS appears by sequence to be a standard unipartite NLS rich in basic residues, there is good reason to expect that a few

adjacent or clustered K/R to A substitutions will abrogate nuclear localization without affecting surrounding protein sequences. Once this is achieved, I will compare the stability of FRQ in cytoplasm vs. in nucleus. By using an epitope tagged versions of the mutant-NLS FRQ, I will be able to compare the stability of the portion of wild type FRQ that remains normally in the cytoplasm to the mutant-NLS FRQ that cannot enter the nucleus.

- Aim 4: If time allows after pursuing the earlier more straightforward experiments, I will define the function of phosphorylation.

As originally described in *Neurospora* and subsequently verified in *Drosophila*, disruption of kinase, CKII (*cka*^{RIP} mutant), leads to arrhythmicity characterized by a stable, hypophosphorylated form of FRQ (or, in *Drosophila*, PER). In the same context of confirming the existence of autocatalysis, it is necessary to investigate the interactions of kinases and monomers vs. dimers, and their subsequent degradations. Recently, it was discovered that degradation of multiply phosphorylated FRQ is mediated by a protein called FWD1, which facilitates FRQ ubiquitylation and proteolysis. However, it is not clear whether both monomers and dimers of FRQ have same proteolysis pathway.

An interesting fact about the above mutant (*cka*^{RIP}) in *Neurospora* is that even in high FRQ level, *frq* message seems to be also high. This contradicts with one's intuitive expectation from the function of negative feedback loop. It has been also shown that FRQ in *cka*^{RIP} mutants actively bind to WCC. In other words, hypophosphorylated FRQ fails to inhibit its own synthesis. This suggests that progressive phosphorylation is required for the activity of FRQ. FRQ becomes active as it gets multiply phosphorylated, and puts itself into the degradation machinery afterwards, providing a small window for self-inhibition. Phosphorylation-related activity of FRQ and its degradation need to be carefully dismantled for clear understanding of circadian rhythms' dynamics in *Neurospora crassa*.

References

1. de Mairan, J.J.D., *Observation botanique*. Historie de l'Academie Royale des Sciences. 1729, Paris. 35.

2. Siffre, M., *Six Months Alone in a Cave.* National Geographic, 1975(March): p. 426-435.

3. Pittendrigh, C.S., *Circadian Clocks: What are They?*, in *The Molecular Basis of Circadian Rhythms*, H. J.W. and S. H., Editors. 1975, Abakon Verlagsgesellschaft: Berlin. p. 11-48.

4. Pittendrigh, C.S., *On Temperature Independence in the Clock System Controlling Emergence Time in Drosophila.* Proc. Natl. Acad. Sci. USA, 1954. 40(10): p. 1018-1029.

5. Brinkmann, K., *Respiration Dependent Types of Temperature Compensation in the Circadian Rhythm of Euglena gracilis*, in *Biological and Biochemical Oscillators*, B. Chance, et al., Editors. 1973, Academic Press: New York and London. p. 513-521.

6. Ruoff, P., et al., *Modeling temperature compensation in chemical and biological oscillators.* Chronobiol. Int., 1997. 14: p. 499-510.

7. Forger, D. and C.S. Peskin, *A Detailed Predictive Model of the Mammalian Circadian Clock.* Proc. Natl. Acad. Sci. USA, 2003: p. in press.

8. Goldbeter, A., *A model for circadian oscillations in the Drosophila PERIOD protein (PER).* Proc. R. Soc. London Ser. B, 1995. 261(1362): p. 319-324.

9. Jewett, M.E., D.B. Forger, and R.E. Kronauer, *Revised Limit Cycle Oscillator Model of Human Circadian Pacemaker.* J. Biol. Rhythms, 1999. 14(6): p. 493-499.

10. Leloup, J. and A. Goldbeter, *A Model for Circadian Rhythms in Drosophila Incorporating the Formation of a Complex between the PER and TIM Proteins.* Journal of Biological Rhythms, 1998. 13(1): p. 70-87.

11. Leloup, J. and A. Goldbeter, *Toward a detailed computational model for the mammalian circadian clock.* Proc. Natl. Acad. Sci. USA, 2003. 100(12): p. 7051-7056.

12. Smolen, P., D.A. Baxter, and J.H. Byrne, *Modeling Circadian Oscillations with Interlocking Positive and Negative Feedback Loops.* The Journal of Neuroscience, 2001. 21(17): p. 6644-6656.

13. Tyson, J.J., et al., *A Simple Model of Circadian Rhythms Based on Dimerization and Proteolysis of PER and TIM.* Biophys. J., 1999. 77: p. 2411-2417.

14. Ueda, H., M. Hagiwara, and H. Kitano, *Robust Oscillations within Two Feedback Model of Drosophila Circadian Rhythm.* J. Theor. Biol., 2001. 210: p. 401-406.

15. Konopka, R.J. and S. Benzer, *Clock Mutants of Drosophila melanogaster.* Proc. Natl. Acad. Sci. USA, 1971. 68(9): p. 2112-2116.

16. Huang, Z.J., K.D. Curtin, and M. Rosbash, *PER Protein Interactions and Temperature Compensation of a Circadian Clock in Drosophila.* Science, 1995. 267: p. 1169-1172.

17. Huang, Z.J., I. Edery, and M. Rosbash, *PAS is a dimerization domain common to Drosophila Period and several transcription factors.* Nature, 1993. 364: p. 259-262.

18. Rutila, J.E., et al., *CYCLE Is a Second bHLH-PAS Clock Protein Essential for Circadian Rhythmicity and Transcription of Drosophila period and timeless.* Cell, 1998. 93: p. 805-814.

19. Bae, K., et al., *dCLOCK Is Present in Limiting Amounts and Likely Mediates Daily Interactions between the dCLOCK-CYC Transcription Factor and the PER-TIM Complex.* Journal of Neuroscience, 2000. 20(5): p. 1746-1753.

20. Darlington, T.K., et al., *Closing the Circadian Loop: CLOCK-Induced Transcription of Its Own Inhibitors per and tim.* Science, 1998. 280: p. 1599-1603.

21. Allada, R., et al., *A Mutant Drosophila Homolog of Mammalian Clock Disrupts Circadian Rhythms and Transcription of period and timeless.* Cell, 1998. 93: p. 791-804.

22. Sehgal, A., et al., *Rhythmic Expression of timeless: A Basis for Promoting Circadian Cycles in period Gene Autoregulation.* Science, 1995. 270: p. 808-810.

23. So, W.V. and M. Rosbash, *Post-transcriptional regulation contributes to Drosophila clock gene mRNA cycling.* EMBO, 1997. 16: p. 7146-7155.

24. Hardin, P.E., J.C. Hall, and M. Rosbash, *Feedback of the Drosophila period gene product of circadian cycling of its messenger RNA levels.* Nature, 1990. 343: p. 536.

25. Zeng, H., P.E. Hardin, and M. Rosbash, *Constitutive overexpression of the Drosophila period protein inhibits mRNA cycling.* EMBO, 1994. 13: p. 3590-3598.

26. Suri, V., A. Lanjuin, and M. Rosbash, *TIMELESS-dependent Positive and Negative Autoregulation in the Drosophila Circadian Clock.* EMBO, 1999. 18(3): p. 675-686.

27. Kloss, B., et al., *The Drosophila Clock Gene double-time Encodes a Protein Closely Related to Human Casein Kinase I.* Cell, 1998. 94: p. 97-107.

28. Price, J.L., et al., *double-time Is a Novel Drosophila Clock Gene that Regulates PERIOD Protein Accumulation.* Cell, 1998. 94: p. 83-95.

29. Kloss, B., et al., *Phosphorylation of PERIOD Is Influenced by Cycling Physical Association of DOUBLE-TIME, PERIOD, and TIMELESS in the Drosophila Clock.* Neuron, 2001. 30: p. 699-706.

30. Sehgal, A., et al., *Loss of Circadian Behavioral Rhythms and per RNA Oscillations in the Drosophila Mutant timeless.* Science, 1994. 263: p. 1603-1606.

31. Myers, M.P., et al., *Positional Cloning and Sequence Analysis of the Drosophila Clock Gene, timeless.* Science, 1995. 270: p. 805-808.

32. Zeng, H., et al., *A Light-Entrainment Mechanism for the Drosophila Circadian Clock.* Nature, 1996. 380(14): p. 129-135.

33. Vosshall, L.B., et al., *Block in Nuclear Localization of period Protein by a Second Clock Mutation, timeless.* Science, 1994. 263: p. 1606-1609.

34. Gekakis, N., et al., *Isolation of timeless by PER Protein Interaction: Defective Interaction Between timeless Protein and Long-Period Mutant PER^{L}.* Science, 1995. 270: p. 811-814.

35. Lee, C., et al., *Resetting the Drosophila Clock by Photic Regulation of PER and a PER-TIM Complex.* Science, 1996. 271: p. 1740-1744.

36. Saez, L. and M.W. Young, *Regulation of Nuclear Entry of the Drosophila Clock Proteins Period and Timeless.* Neuron, 1996. 17: p. 911-920.

37. Rothenfluh, A., M.W. Young, and L. Saez, *A TIMELESS-Independent Function for PERIOD Proteins in the Drosophila Clock.* Neuron, 2000. 26: p. 505-514.

38. Rothenfluh, A., et al., *Isolation and Analysis of Six timeless Alleles That Cause Short- or Long-Period Circadian Rhythms in Drosophila.* Genetics, 2000. 156: p. 665-675.

39. Martinek, S., et al., *A Role for the Segment Polarity Gene shaggy/GSK-3 in the Drosophila Circadian Clock.* Cell, 2001. 105: p. 769-779.

40. Cashmore, A.R., et al., *Cryptochromes: Blue Light Recptors for Plants and Animals.* Science, 1999. 284: p. 760-765.

41. Ceriani, M.F., et al., *Light-Dependent Sequestration of TIMELESS by CRYPTOCHROME.* Science, 1999. 285: p. 553-556.

42. Emery, P., et al., *CRY, a Drosophila Clock and Light-Regulated Cryptochrome, Is a Major Contributor to Circadian Rhythm Resetting and Photosensitivity.* Cell, 1998. 95: p. 669-679.

43. Emery, P., et al., *Drosophila CRY Is a Deep Brain Circadian Photoreceptor.* Neuron, 2000. 26: p. 493-504.

44. Stanewsky, R., et al., *The cryb Mutation Identifies Cryptochrome as a Circadian Photoreceptor in Drosophila.* Cell, 1998. 95: p. 681-692.

45. Darlington, T.K., et al., *The period E-box Is Sufficient to Drive Circadian Oscillation of Transcription In Vivo.* Journal of Biological Rhythms, 2000. 15(5): p. 462-470.

46. Kyriacou, C.P. and E. Rosato, *Squaing Up the E-box.* Journal of Biological Rhythms, 2000. 15(6): p. 483-490.

47. Bae, K., et al., *Circadian Regulation of a Drosophila Homolog of the Mammalian Clock Gene: PER and TIM Function as Positive Regulators.* Molecular and Cellular Biology, 1998. 18(10): p. 6142-6151.

48. Lee, C., K. Bae, and I. Edery, *The Drosophila CLOCK Protein Undergoes Daily Rhythms in Abundance, Phosphorylation, and interactions with the PER-TIM Complex.* Neuron, 1998. 21: p. 857-867.

49. Glossop, N.R.J., L.C. Lyons, and P.E. Hardin, *Interlocked Feedback Loops Within the Drosophila Circadian Oscillator.* Science, 1999. 286: p. 766-768.

50. Blau, J. and M.W. Young, *Cycling vrille Expression Is Required for a Functional Drosophila Clock.* Cell, 1999. 99: p. 661-671.

51. Cyran, S.A., et al., *vrille, Pdp1, and dClock Form a Second Feedback Loop in the Drosophila Circadian Clock.* Cell, 2003. 112: p. 329-341.

52. Tyson, J.J., et al., *Mathematical Background Group Report*, in *The Molecular Basis of Circadian Rhythms*, S. Bernhard, Editor. 1975, Dahlem Konferenzen: Berlin.

53. Winfree, A.T., *The Geometry of Biological Time*. Biomathematics. Vol. 8. 1980, New York: Springer-Verlag.

54. Strogatz, S.H., *The Mathematical Structure of the Human Sleep-Wake Cycle*. Lecture Notes in Biomathematics, ed. S. Levin. Vol. 69. 1986, New York: Springer-Verlag.

55. Ermentrout, B., *Simulating, Analyzing, and Animating Dynamical Systems*, ed. J.J. Dongarra. 2002, Philadelphia: SIAM.

56. Myers, M.P., et al., *Light-Induced Degradation of TIMELESS and Entrainment of the Drosophila Circadian Clock.* Science, 1996. 271: p. 1736.

57. Kuznetsov, Y.A., *Elements of Applied Bifurcation Theory*. Second ed, ed. J.E. Marsden and L. Sirovich. 1998, New York: Springer.

58. Tyson, J.J., A. Csikasz-Nagy, and B. Novak, *The dynamics of cell cycle regulation.* BioEssays, 2002. 24: p. 1095-1109.

59. Aronson, B.D., K.A. Johnson, and J.C. Dunlap, *Circadian clock locus frequency: protein encoded by a single open reading frame defines period length and temperature compensation.* Proc. Natl. Acad. Sci. USA, 1994. 91: p. 7683-7687.

60. Renn, S.C.P., et al., *A pdf Neuropeptide Gene Mutation and Ablation of PDF Neurons Each Cause Severe Abnormalities of Behavioral Circadian Rhythms in Drosophila.* Cell, 1999. 99: p. 791-802.

61. Helfrich-Foster, C., et al., E*ctopic Expression of the Neuropeptide Pigment-Dispersing Factor Alters Behavioral Rhythms in Drosophila melanogaster.* Journal of Neuroscience, 2000. 20(9): p. 3339-3353.

62. McDonald, M.J. and M. Rosbash, M*icroarray Analysis and Organization of Circadian Gene Expression in Drosophila.* Cell, 2001. 107: p. 567-578.

63. Aronson, B.D., et al., N*egative Feedback Defining a Circadian Clock: Autoregulation of the Clock Gene frequency.* Science, 1994. 263: p. 1578-1584.

64. Cheng, P., et al., P*AS Domain-Mediated WC-1/WC-2 Interaction Is Essential for Maintaining the Steady-State Level of WC-1 and the Function of Both Proteins in Circadian Clock and Light Response of Neurospora.* Molecular and Cellular Biology, 2002. 22(2): p. 517-524.

65. Luo, C., J.J. Loros, and J. Dunlap, N*uclear Localization Is Required for Function for the Essential Clock Protein FRQ.* EMBO, 1998. 17(5): p. 1228-1235.

66. Liu, Y., J. Loros, and J.C. Dunlap, P*hosphorylation of the Neurospora clock protein FREQUENCY determines its degradation rate and strongly influences the period length of the circadian clock.* PNAS, 1999. 97(1): p. 234-239.

67. Yang, Y., P. Cheng, and Y. Liu, R*egulation of the Neurospora circadian clock by casein kinase II.* Genes & Development, 2002. 16: p. 994-1006.

68. Cheng, P., et al., C*oiled-coil domain-mediated FRQ-FRQ interaction is essential for its circadian clock function in Neurospora.* The EMBO Journal, 2001. 20(1 & 2): p. 101-108.

Vitae

Name: Christian I. Hong

Phone: 540-552-9303, 540-231-5958 **Email:** ihong@vt.edu

Address: 1216 University City Blvd. C31
Blacksburg, VA 24060 **Citizenship**: U.S.

Birthdate: February 7th, 1974 **Birthplace:** Seoul, Korea

Academic Degrees

- Ph.D., Biology, Virginia Polytechnic Institute & State University, Expected in Dec. 2003
- M.S., Biology, Virginia Polytechnic Institute & State University, May 1999
  Thesis: Mathematical Modeling of Circadian Rhythms In *Drosophila melanogaster*
- B.S., Biology, Virginia Polytechnic Institute & State University, May 1997
  In Honors, Thesis: A Proposal For Temperature Compensation of the Circadian Rhythm In *Drosophila* Based On Dimerization of the PER Protein

Professional Experience

Paper Reviews

- Reviewed two articles for Journal of Theoretical Biology (one in May and one in September, 2003)
- Reviewed one article for Biophysical Journal (November, 2003)

Invited Talks

- Seminar presentation at the Kavli Institute for Theoretical Physics (KITP) on Biological Networks Workshop at UCSB (March 24 – 29, 2003)
- Seminar presentation, Society for Research on Biological Rhythms (SRBR) Conference (May 22 – 26, 2002)
- Molecular and Cell Biology and Biotechnology seminar presentation with Dr. John Tyson (March 26th, 1999) at Virginia Tech. I presented the molecular biology of circadian rhythms in *Drosophila melanogaster*, and Dr. Tyson presented the modeling of circadian clock mechanism.

Poster Presentations

- Biology Department Research day (Sept. 19th, 2003)
- Gordon Research Conference (GRC) in Theoretical Biology & Biomathematics (June 9 – 14, 2002)
- Virginia Tech Workshop of Bioinformatics and Computational Biology (March 19th, 2001)
- The Society for Mathematical Biology (SMB) 2000 Conference (Aug. 3rd, 2000 – Aug. 5th, 2000)
- Gordon Research Conference in (GRC) Theoretical Biology (June 11th, 2000 – June 16th, 2000)
- The 15th Annual Research Symposium at Virginia Tech (March 29th, 1999)

Assistantships and Fellowships

- Junior Fellow at Collegium Budapest, Institute for Advanced Study in Budapest, Hungary (Feb. – July 2003)
- Graduate Research Assistantship (Summer of 1998, 1999, 2000, 2001, Jan. – Dec. 2002, Fall 2003)
- Graduate Teaching Assistantship (Fall & Spring of 1997 – 2001)

Teaching Experiences

- Principles of Biology Laboratory Classes, taught three classes each semester with full responsibility of teaching, giving exams, and grades (Fall 1997 – Fall 2001)

Professional Memberships

- Member, the Society for Mathematical Biology (June 2000 – present)
- Assistant staff, Korea Campus Crusade for Christ at Virginia Tech (Spring, 1999 – present)
- President, Korea Campus Crusade for Christ at Virginia Tech (Aug. 1996 – May 1997)
- Member, University Honors Association
- Member, Golden Key National Honor Society
- Member, Gamma Beta Phi National Honor Society
- Member, Phi Eta Sigma National Honor Society

Publications

- Hong, C.I., Novak, B., & Tyson, J.J. A Proposal for Robust Temperature Compensation of Circadian Rhythms (submitted to PNAS, Nov. 2003)
- Tyson, J.J., Hong, C.I., Thron, D., & Novak, B. A Simple Model of Circadian Rhythms Based on Dimerization And Proteolysis of PER and TIM, Biophysical Journal, 1999; 77: 2411-2417.
- Hong, C.I. & Tyson, J.J. A Proposal for Temperature compensation of the Circadian Rhythm in *Drosophila* Based on Dimerization of the PER Protein, Chronobiology International 1997; 14(5): 521-529.

Community Services

- Volunteer at Crisis Pregnancy Center of the New River Valley (April 1995 – Dec. 1998)

Reference

- Dr. Tyson, John J. (Advisor), tyson@vt.edu
  Department of Biology, 2097 Derring Hall, Virginia Tech, Blacksburg, VA 24060, Tel.: 540-231-4662, Fax: 540-231-9307
- Dr. Novak, Bela, bnovak@mail.bme.hu
  Department of Agricultural Chemical Technology, Budapest University of Technology and Economics, Budapest 1521 Hungary